IRRADIATION EFFECTS ON MICROSTRUCTURAL EVOLUTION

Grace Burke, University of Manchester
Wade Karlsen, VTT

The University of Manchester
Materials Performance Centre

This project received funding under the Euratom research and training programme 2014-2018 under grant agreement N° 661913

Introduction

- An important objective of SOTERIA Task 4.1 and D4.1 is to gain a better understanding of neutron-irradiation effects, and relate that to the efforts to make predictive models of IASCC.
- At the SOTERIA Mid-Term Seminar, low-dpa (proton and neutron)damage phenomena and the manifestation of localized deformation were illustrated through TEM and STEM-EDX microanalysis data.
- An important objective in SOTERIA Tasks 4.3 and 4.4 is to explore irradiation's role in promoting IASCC in the high dpa regime, through autoclave testing of O-ring specimens of highly-irradiated flux thimble tube material in simulated PWR environment.
- This presentation describes irradiation-induced phenomena occurring at dpa levels (5 and above) that may make materials susceptible to IASCC after significant dose accumulation, so important for long-term operation of nuclear power plants.

WP 4: TASK4.1.1

Microstructural Characterization of Proton-Irradiated Type 316L SS

Grace Burke, Elisabeth Francis, Liberato Volpe, Kudzanai Mukahiwa and Jonathan Duff (University of Manchester)

* Ovidiu Toader / Gary Was (MIBL)

The University of Manchester
Materials Performance Centre

This project received funding under the Euratom research and training programme 2014-2018 under grant agreement N° 661913

OUTLINE

- Materials/Proton Irradiation
- Characterization Techniques
- Results
  - As-Received 316L
  - As-Proton-Irradiated 316L
  - Post-IASCC Characterization Approach

Material: Type 316L SS (Framatome)

- Non-irradiated 316L SS Properties:

Chemical Composition

Wt. %	C	S	P	Si	Mn	Ni	Cr	Mo	Cu
316L	0.023	0.008	0.025	0.488	1.73	12.31	17.52	2.45	0.132

Room Temperature Mechanical Properties

Temp.	σ_y (Mpa)	UTS (Mpa)	RA%	Hardness (Hv)
RT	279	584	56.5	150

Microstructural Properties

Material	Heat	Ms (°C)	Md30 (°C)	Grain Size (μm)	Ferrite (%)	SFE (mJ/m²)
316L	T8289	-224	-7.2	125	3.3	30.4

Proton Irradiation

- Proton irradiation of Framatome 316L SS performed at the University of Michigan Ion Beam Laboratory (MIBL)
- Irradiation at 350°C to dose of 5 dpa (~12µm depth- SRIM) at a flux of ~1.15 X 10^{-5} dpa/s across central 10 mm of samples (used for IASCC 4 pt bend tests)
- Characterisation to assess damage and RIS

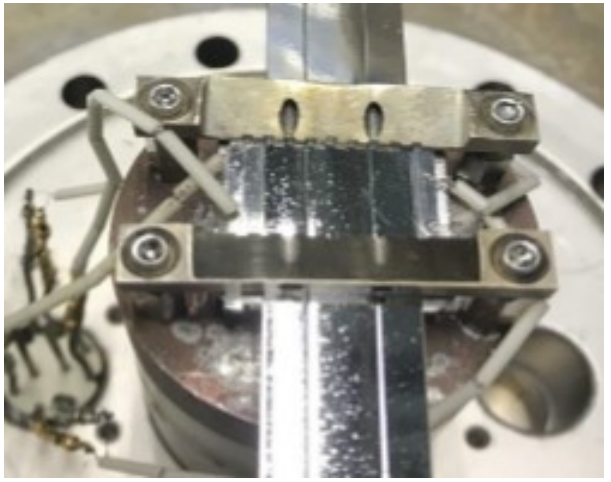

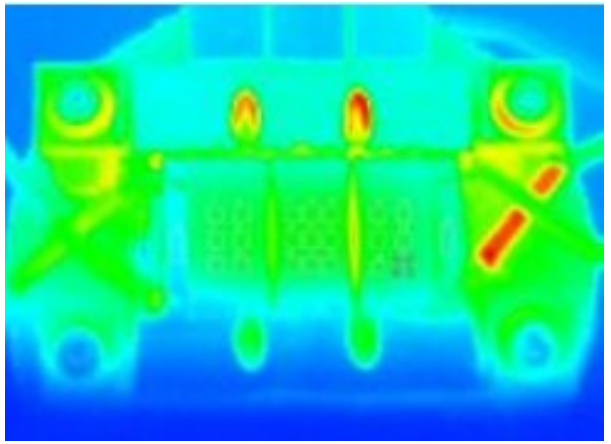

Microstructural Characterization

- General microstructural characterization (as-received, proton-irradiated, post-IASCC tested specimens)
  - FEG-SEM (SE and BSE Imaging) and SEM-EDX Spectrum Imaging: **Zeiss Merlin** with Oxford Instruments Xmax Extreme low voltage SDD and 2 XMax 150 SDDs with an AZTEC analysis system.
- TEM and AEM Characterization (as-received and proton-irradiated electropolished specimens)
  - **Philips CM20** TEM
  - **FEI Talos F200 S/TEM** with X-FEG and Super X (4 SDDs) EDX analysis system (Velox 2 software)
- TEM/AEM Specimen preparation:
  - Mechanically thinned from "backside" to ~100 μm
  - "Dimpled" from backside to <20 μm
  - Conventional twin jet electropolish (Struers Tenupol)

Non-Irradiated 316L SS: TEM

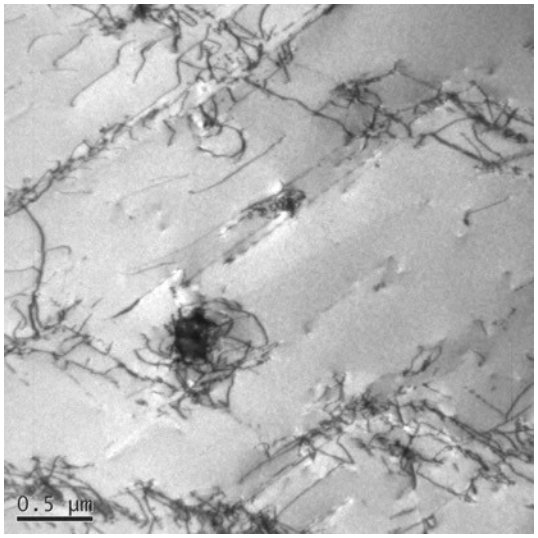

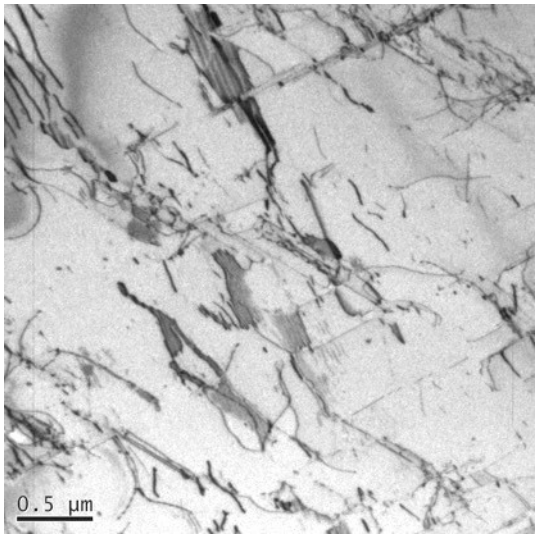

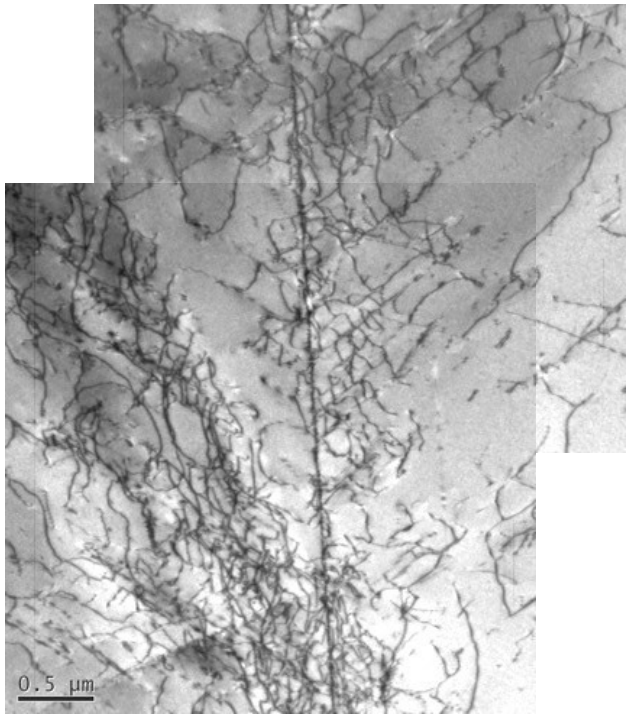

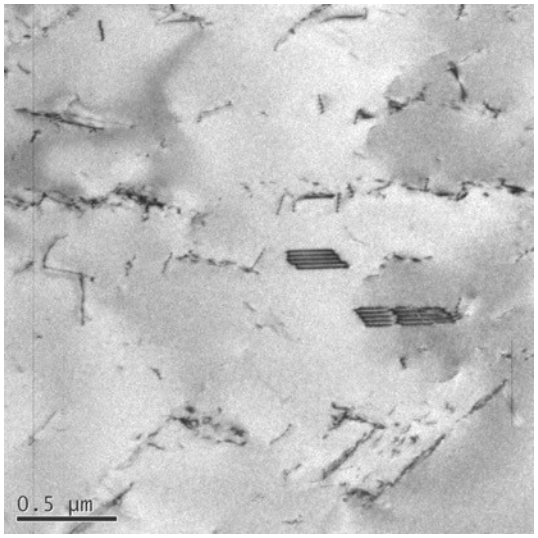

- General microstructure: Recrystallized grains; some evidence of intermediate T deformation (polygonization)
- No intergranular precipitation detected
- Numerous banded inclusions (complex silicates/MnS)

Non-Irradiated 316L SS: GB Segregation

BF STEM + Elemental maps from STEM-EDX SI Datasets

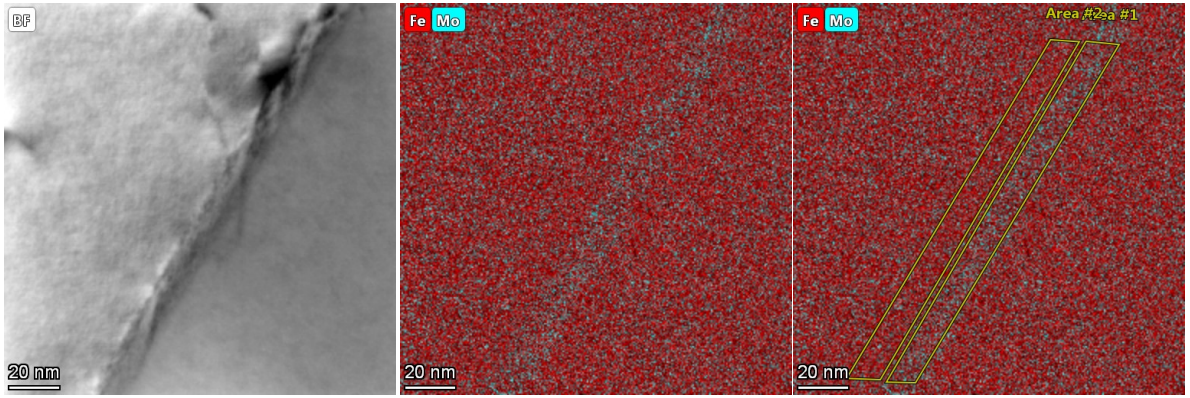

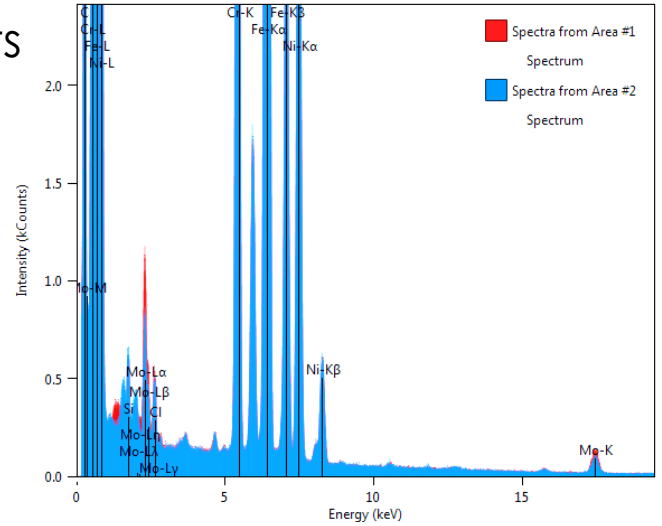

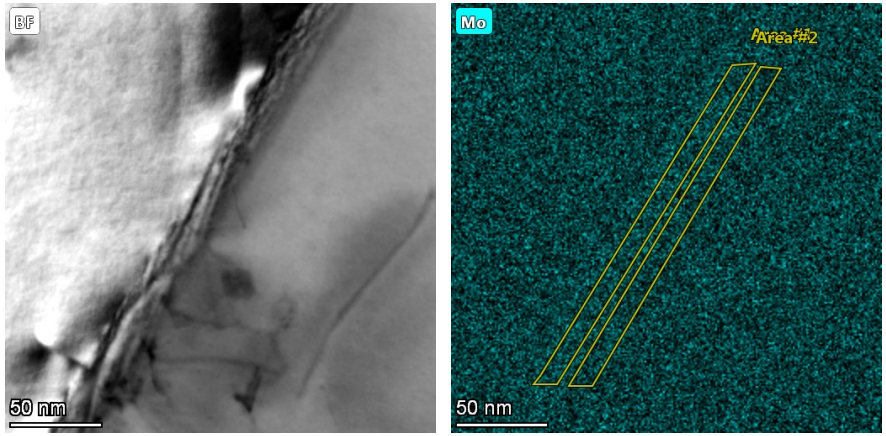

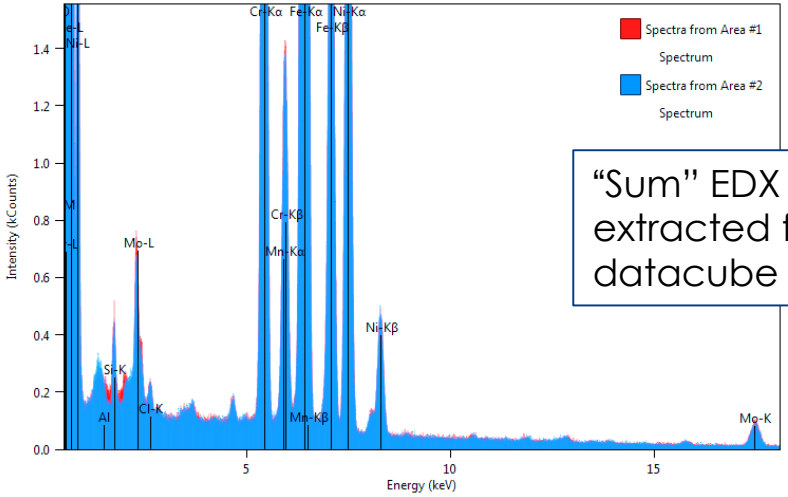

"Sum" EDX spectra extracted from SI datacube

- Inclined grain boundary: detectable Mo segregation in as-received condition (Consistent along grain boundary)

Non-Irradiated 316L SS: GB Segregation

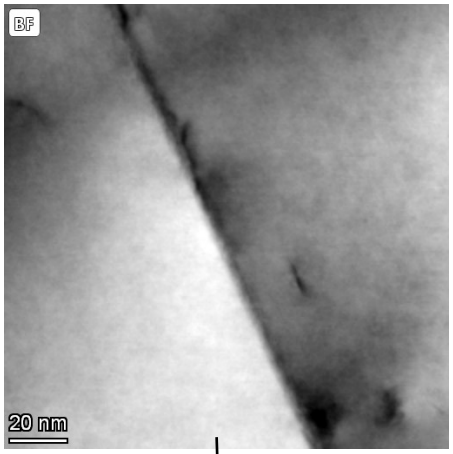

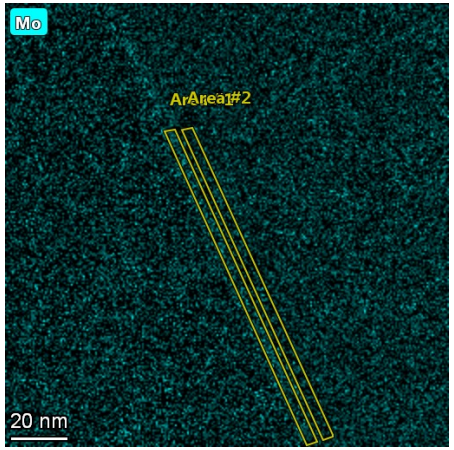

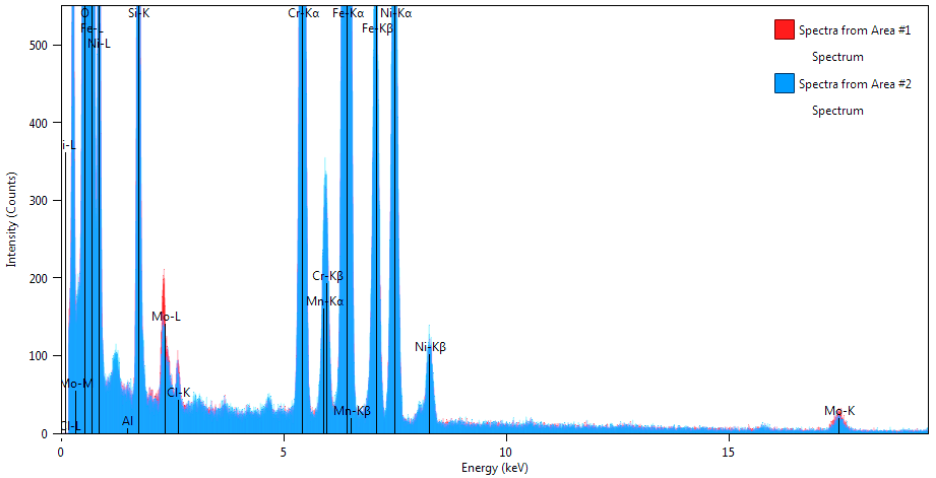

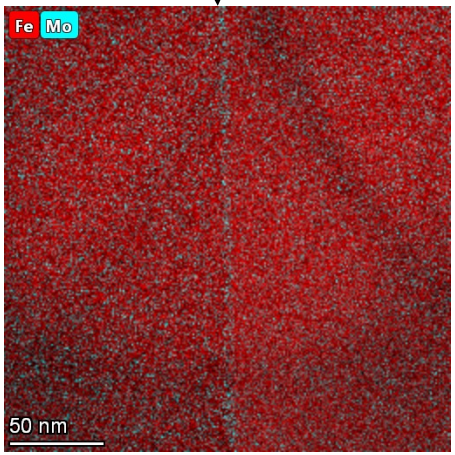

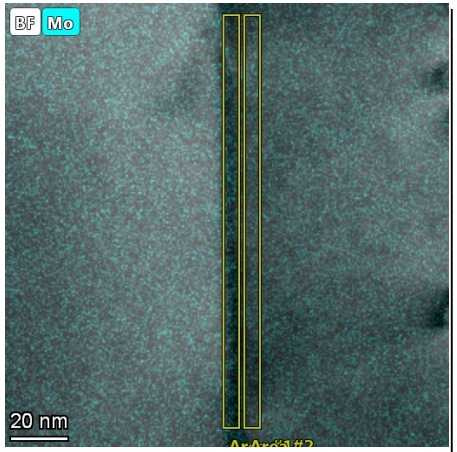

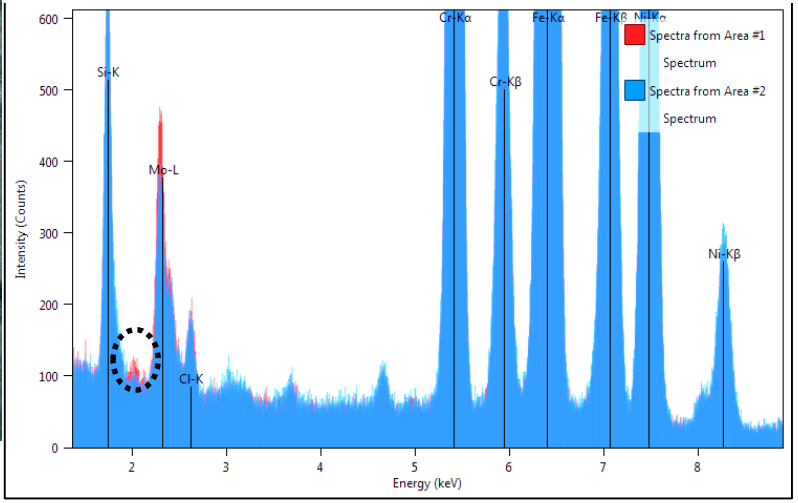

"Lower" magnification:
Fe+Mo maps

- Detectable intergranular Mo segregation in as-received condition
- Confined to grain boundaries

Proton-Irradiated 316L SS: 5 dpa at 350°C

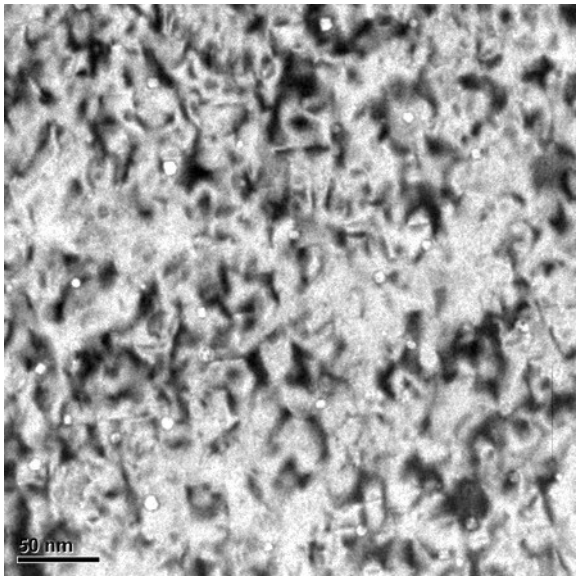

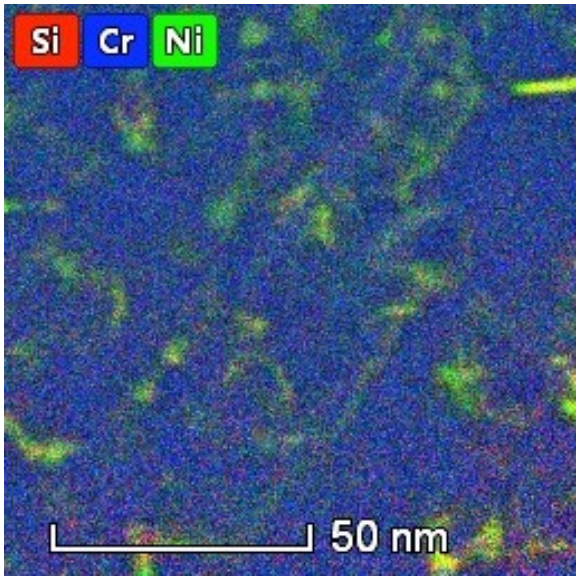

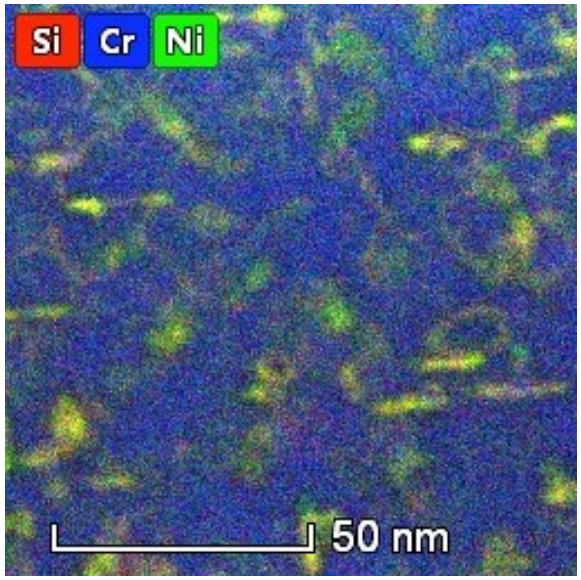

From April 2018 Mid-Term Seminar/Workshop:

- Proton irradiation-induced cavities ranging from ~5 to ~10 nm in diameter
- Proton irradiation-induced Frank loops
- Proton irradiation-induced segregation of Si and Ni to loops, cavity-metal interfaces, and pre-existing dislocation

Proton-Irradiated 316L SS: 5 dpa at 350°C

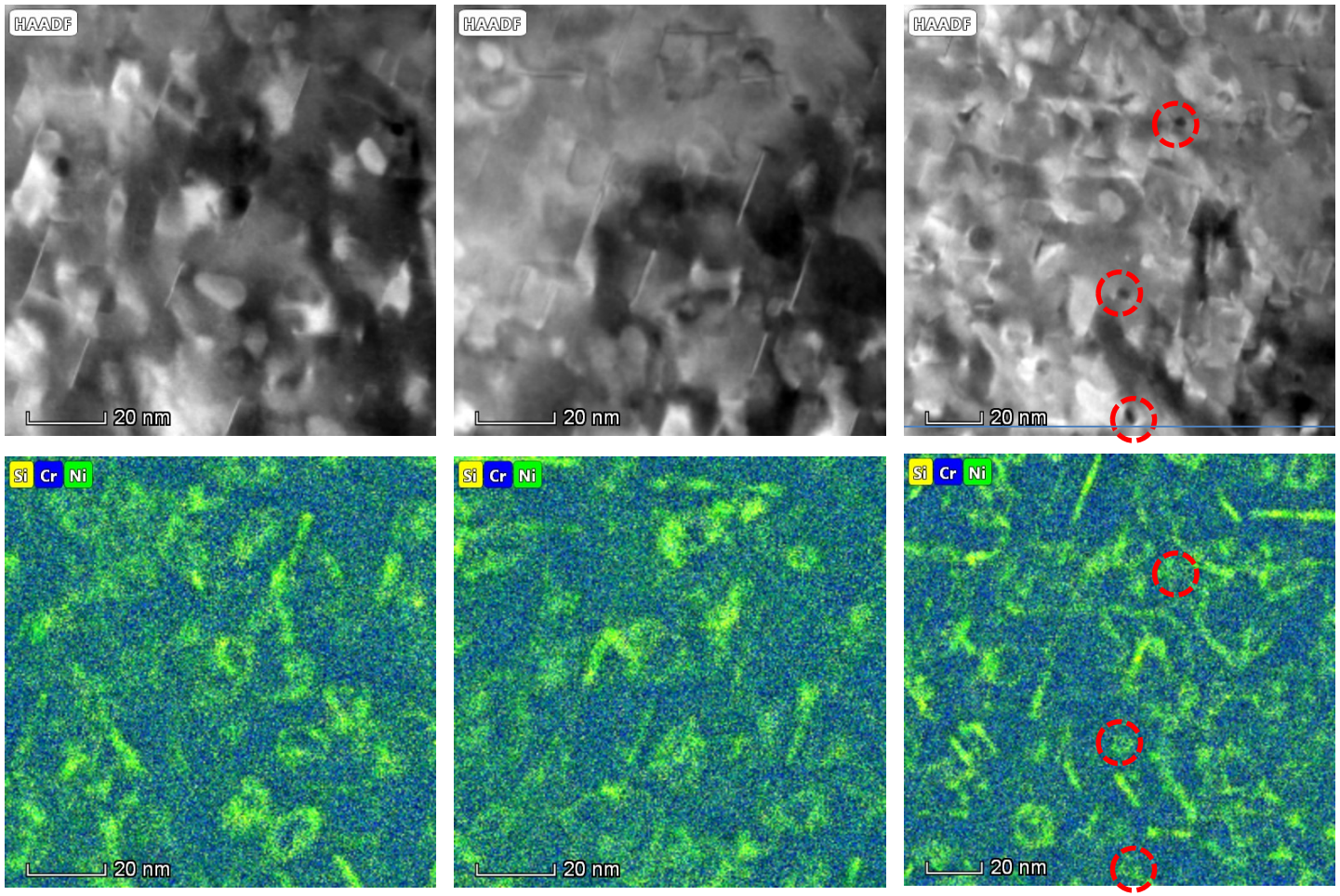

- Clear Ni and Si segregation to loops, nano-scale cavities and pre-existing dislocations (Note ability to detect "out of contrast" dislocations/loops)

Proton-Irradiated 316L SS: 5 dpa at 350°C

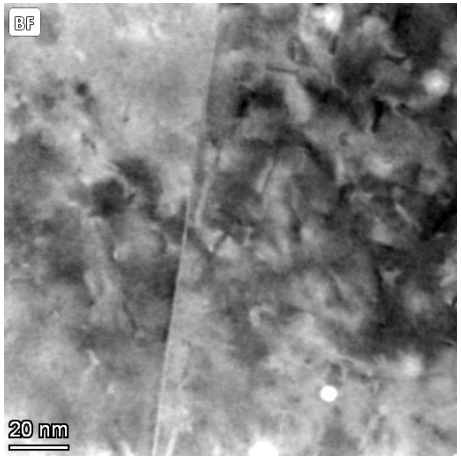

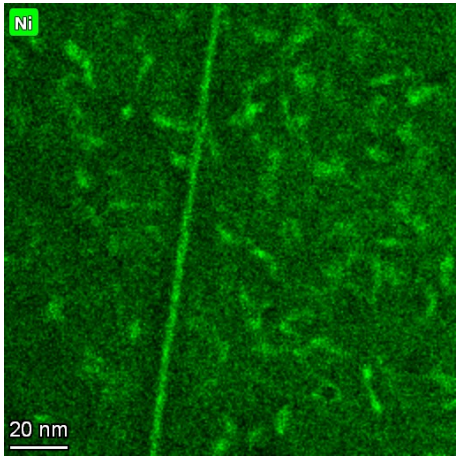

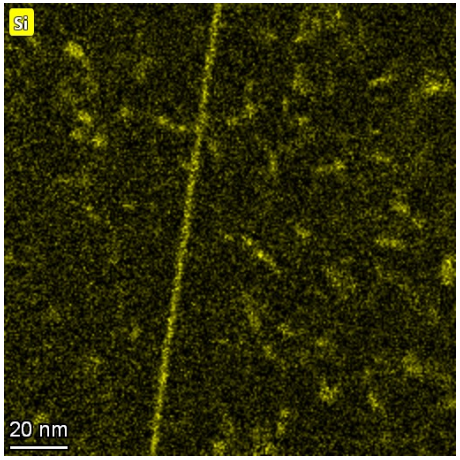

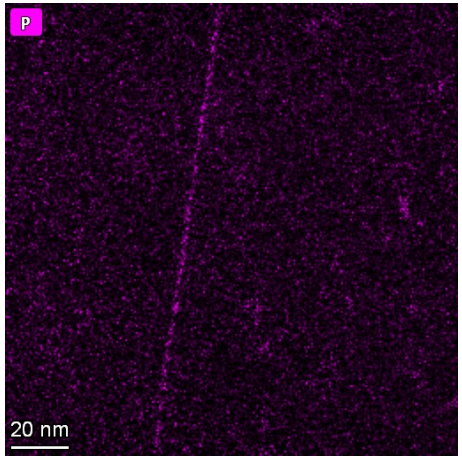

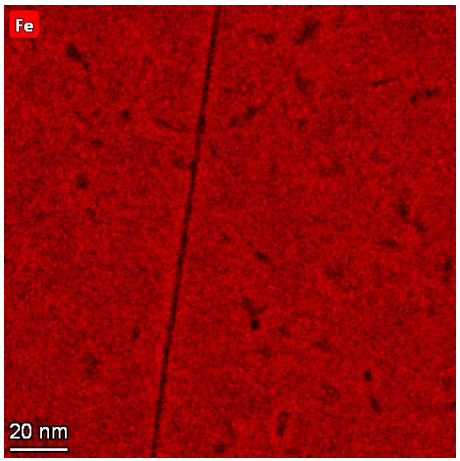

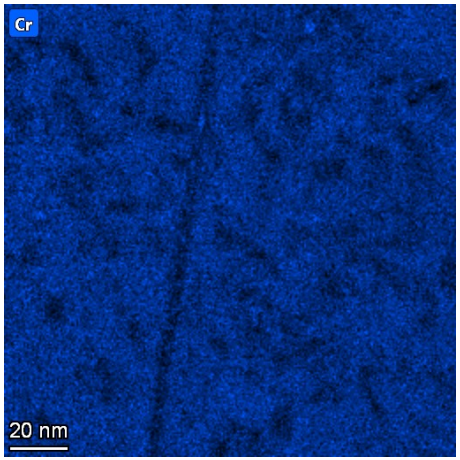

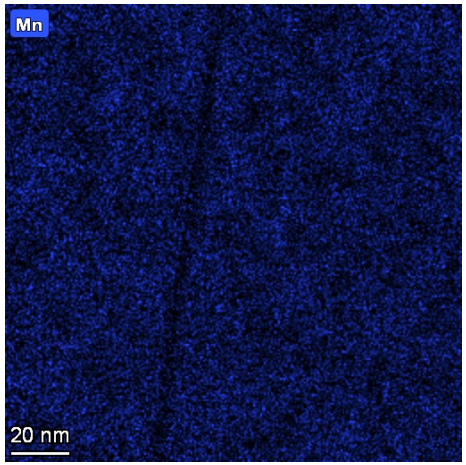

- Proton-irradiation-induced segregation to irradiation-induced defects (loops/nano-scale cavities), pre-existing dislocations and grain boundaries

Proton-Irradiated 316L SS: 5 dpa at 350°C

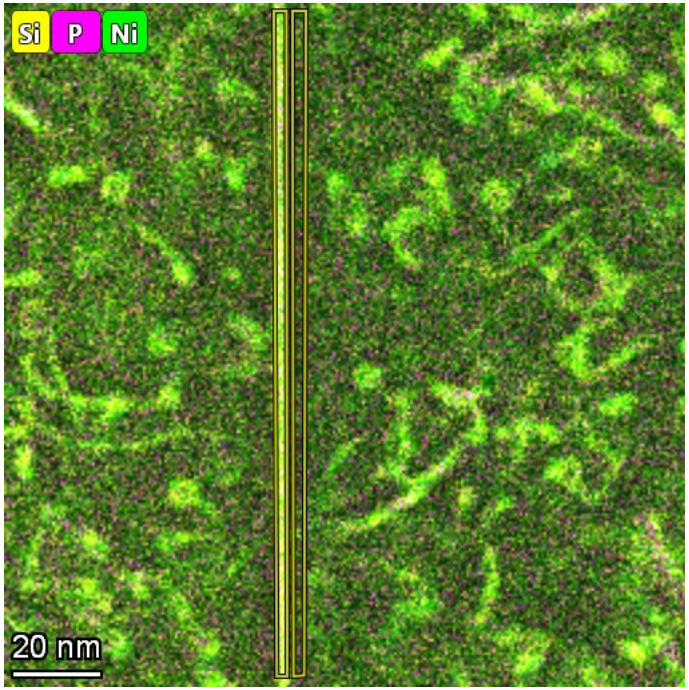

"Sum" EDX spectra extracted from SI datacube

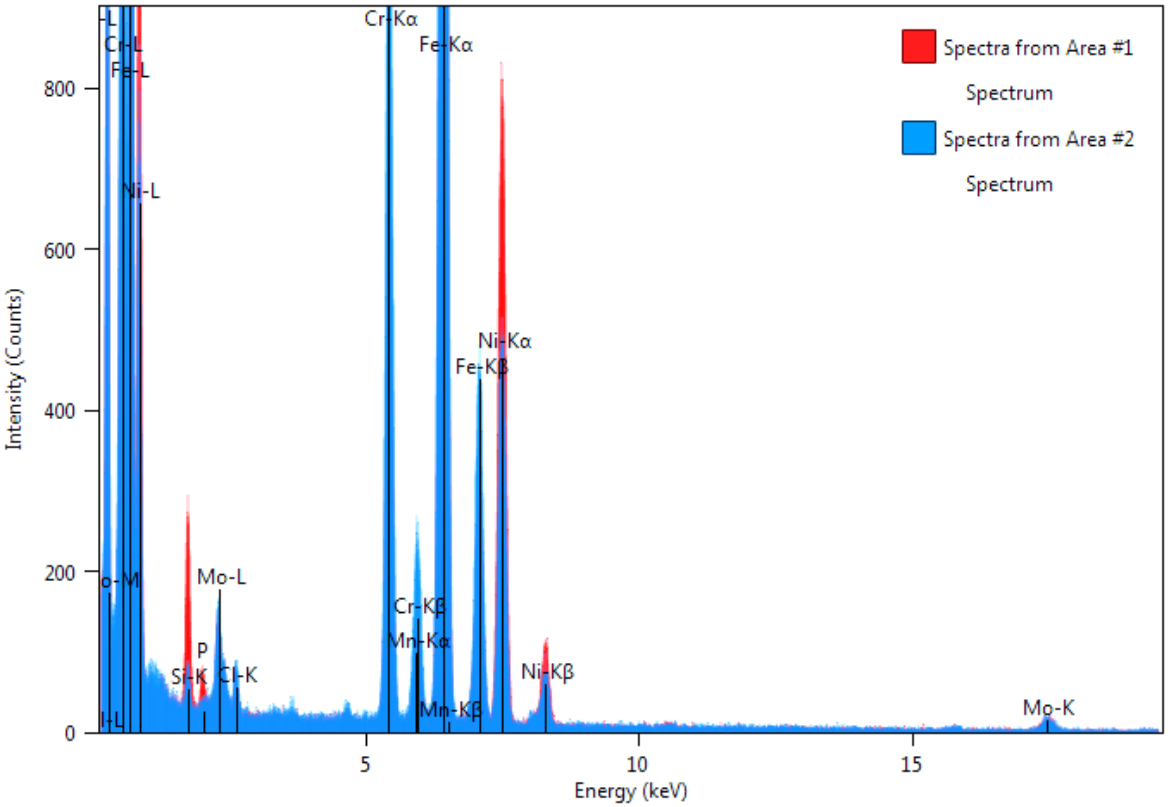

- Extensive defect formation: Frank loops, nano-scale cavities
- Extensive RIS: Grain boundaries, pre-existing dislocations, irradiation-induced defects
- **Intergranular RIS: Si, Ni and P (No Mo)**

Proton-Irradiated 316L SS: 5 dpa at 350°C

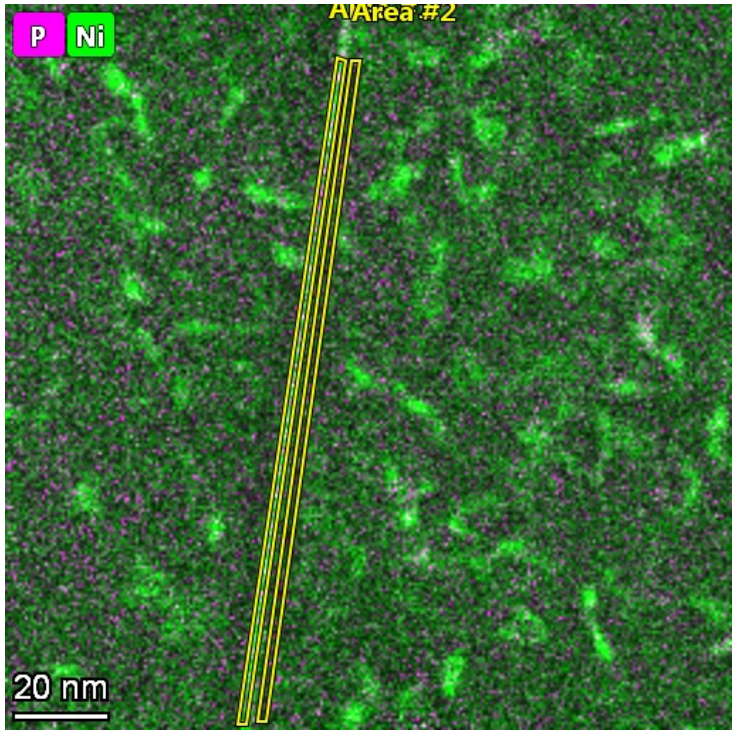

"Sum" EDX spectra extracted from SI datacube

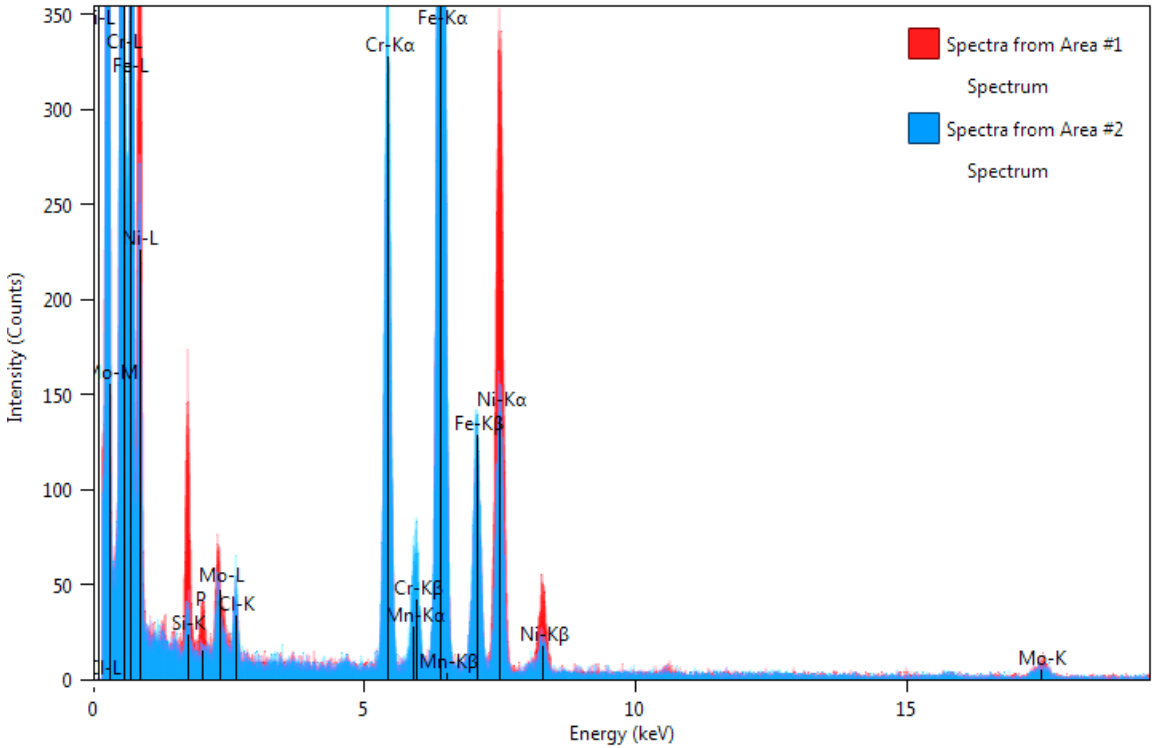

- STEM-EDX SI dataset analysis: Significant enrichments of Si, P and Ni at grain boundaries
- Mo segregation similar to non-irradiated

Proton-Irradiated 316L SS: Post-Test Analysis

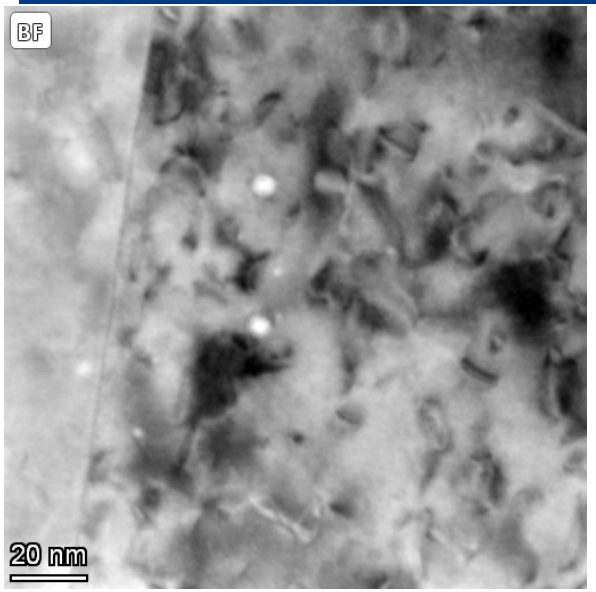

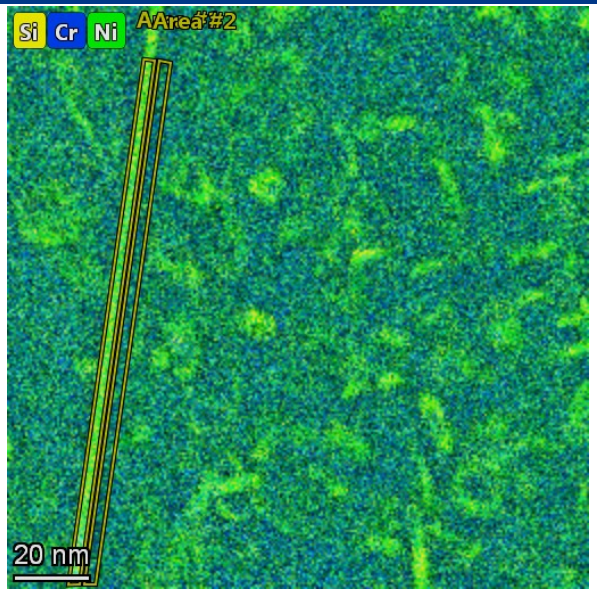

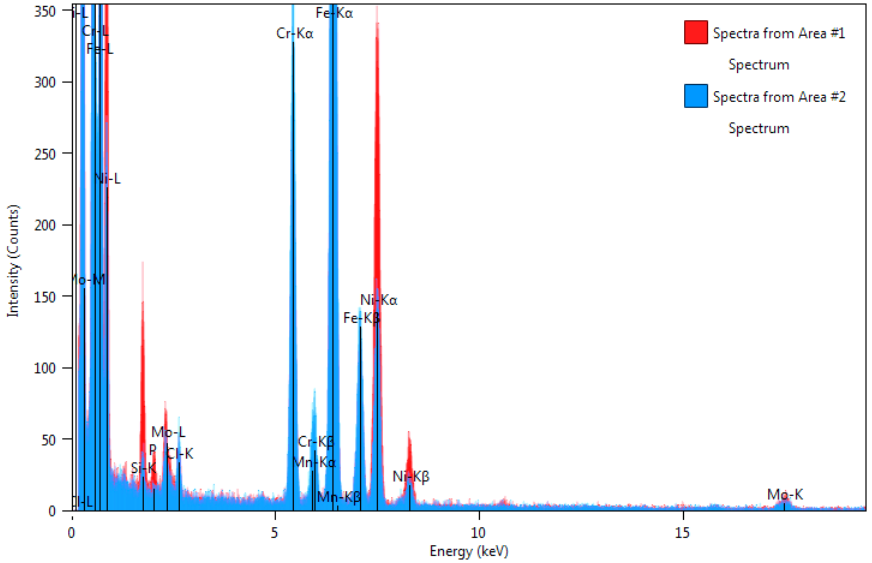

- Pronounced intergranular Si and Ni (and P) segregation
- Segregation of Si and Ni to nano-scale irradiation-induced cavities, loops, and pre-existing dislocations
- Elevated Mo levels at boundary (similar to non-irradiated)

316L SS Microstructure Summary

As-Received

- Intergranular segregation of Mo to grain boundaries
- No evidence of intergranular precipitation
- Numerous oxide and MnS inclusions (banded)

As-Proton-Irradiated

- Formation of Frank Loops and nano-scale (~5 to 10 nm diameter) cavities; density = ~1 X $10^{22}/m^3$
- Extensive RIS of Si, P and Ni to grain boundaries (Mo present)
- Extensive segregation of Si and Ni to Frank Loops, nano-scale cavity/matrix interfaces, and pre-existing dislocations
- Estimated density of Ni-Si "segregated features" is ~6 to ~9 X$10^{22}/m^3$
- "Quantification" of STEM-EDX SI data and discrete "spot" analyses in progress (new Velox software).

Proton-Irradiated 316L SS: Post-Test Analysis

Task 4.4.1 IASCC (To be presented by Sarah Sherry (Wood) and Jonathan Duff (University of Manchester – MPC)

Post-Test metallographic cross-section specimens prepared for FEG-SEM characterization

- Crack length measurements
- FEG-SEM EDX SI evaluation (Low Voltage SEM-EDX SI to improve spatial resolution: 3.5 to 5 kV)

Specimen Preparation

- Metallographic grinding (SiC papers) and polishing
- Vibromat (no chemical etching)

Proton-Irradiated 316L SS: Post-Test Analysis

BSE Imaging: IASCC 4 pt Bend Specimens

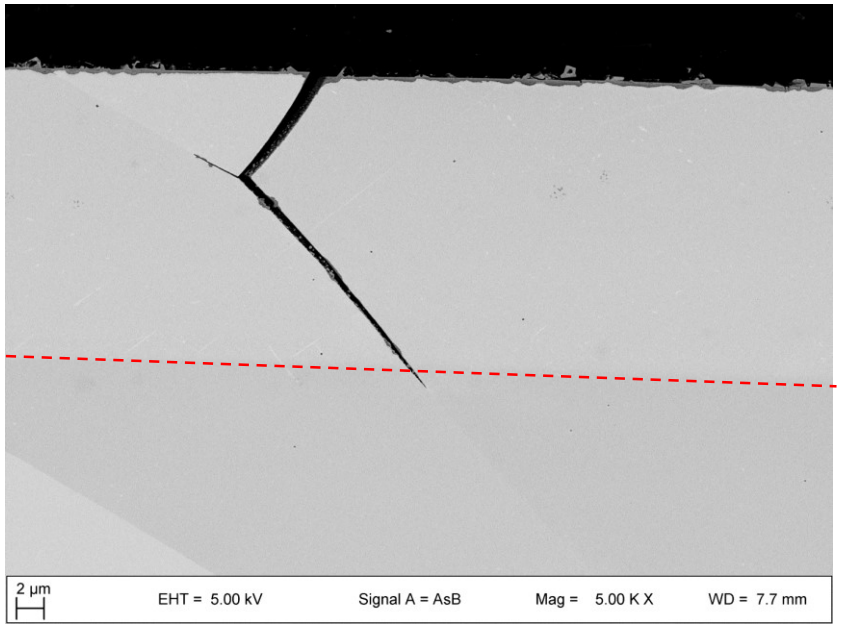

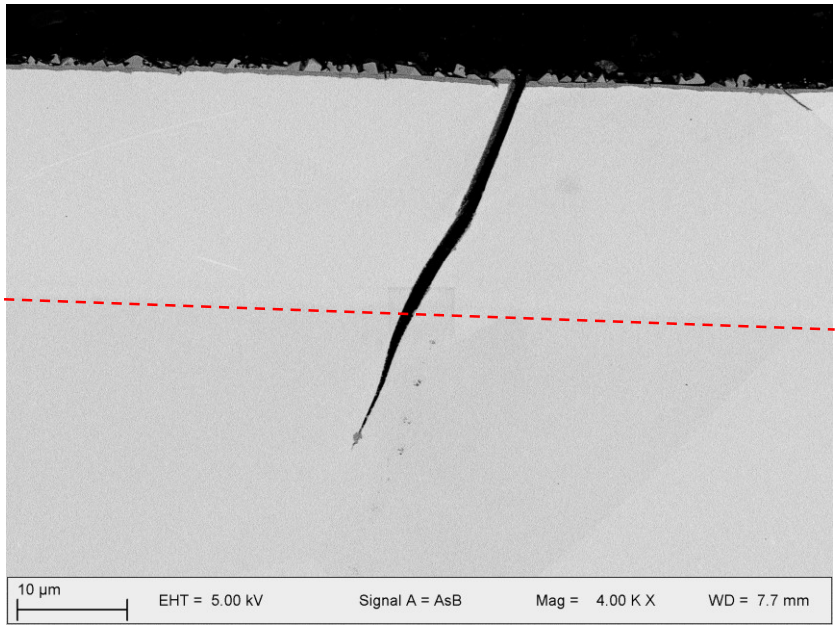

- Discernable BSE contrast difference between the proton-irradiated "layer" and the non-irradiated "base"

Proton-Irradiated 316L SS: Post-Test Analysis

5 kV FEGSEM-EDX Spectrum Imaging Analysis (~70 nm depth resolution)

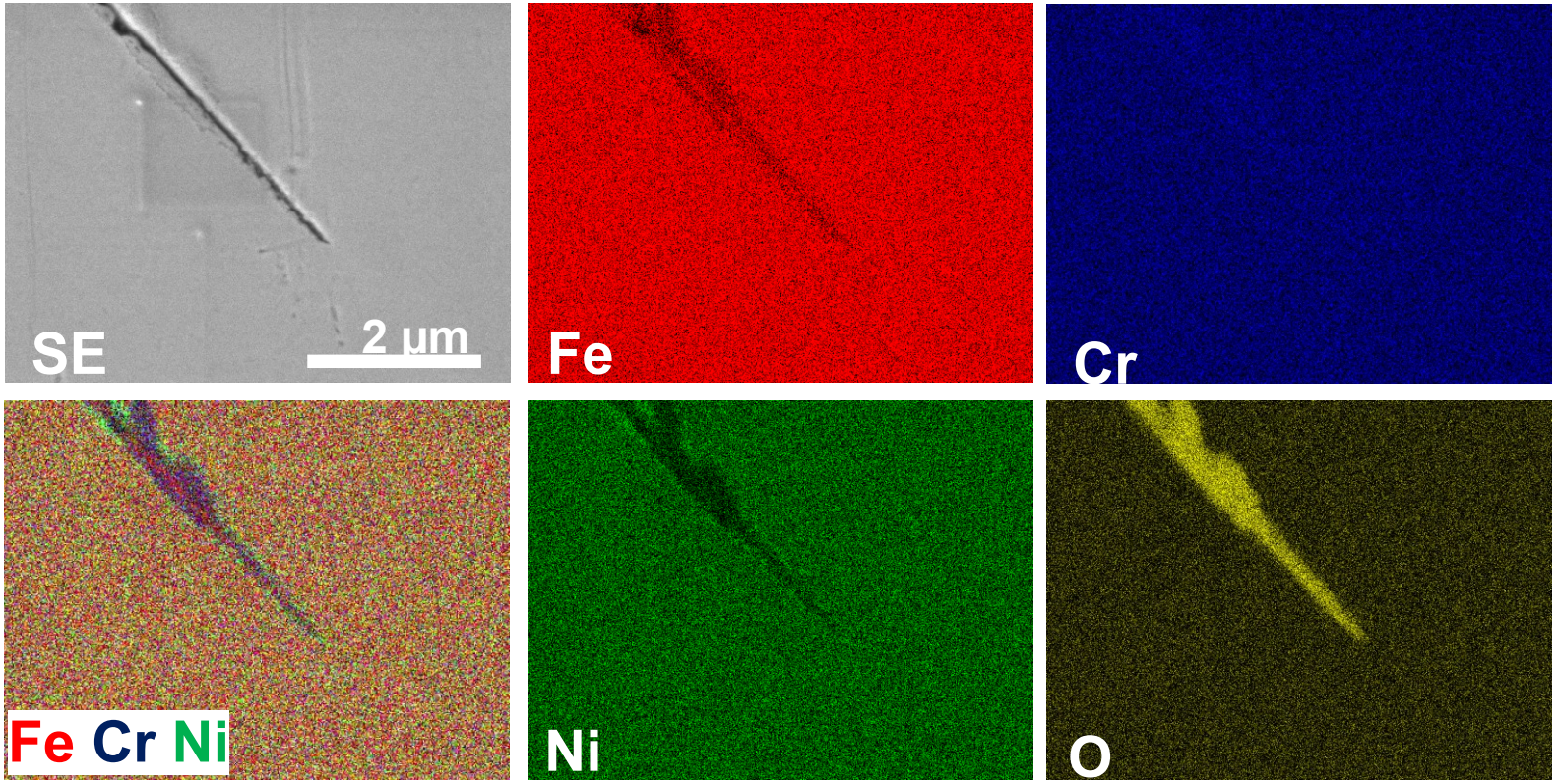

- Oxide present within crack; Ni enrichment in vicinity of oxide/metal interface

Proton-Irradiated 316L SS: Post-Test Analysis

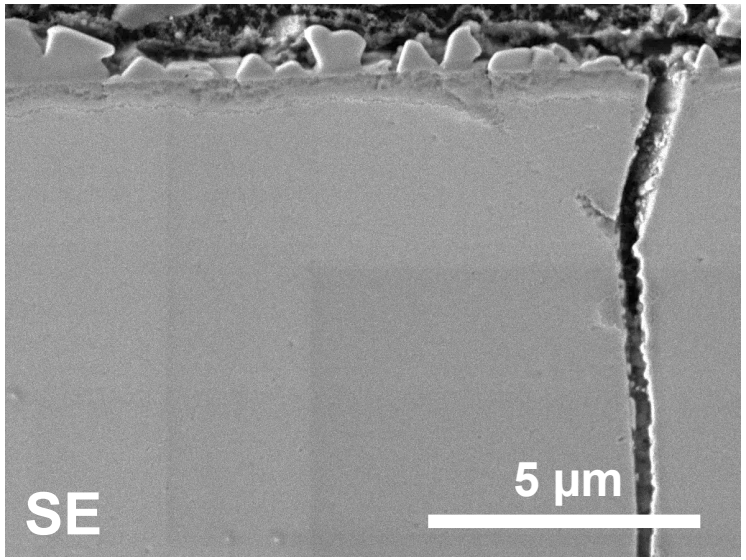

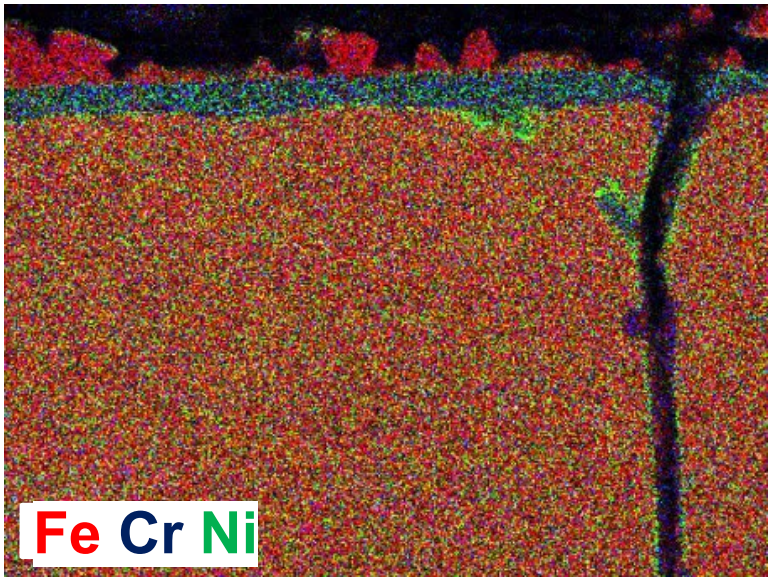

10 kV analyses (X-Max 150 SDD)

- Oxide present within crack; Ni enrichment in vicinity of oxide/metal interface

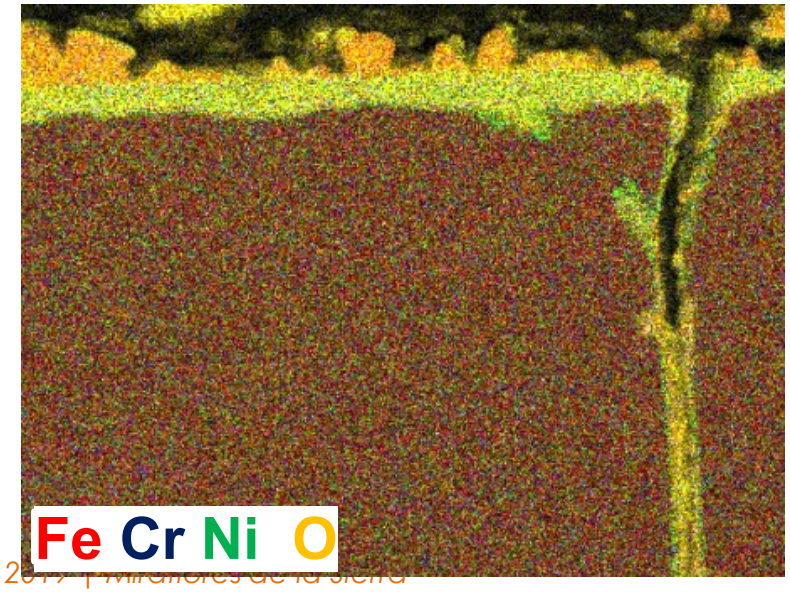

Proton-Irradiated 316L SS: Post-Test Analysis

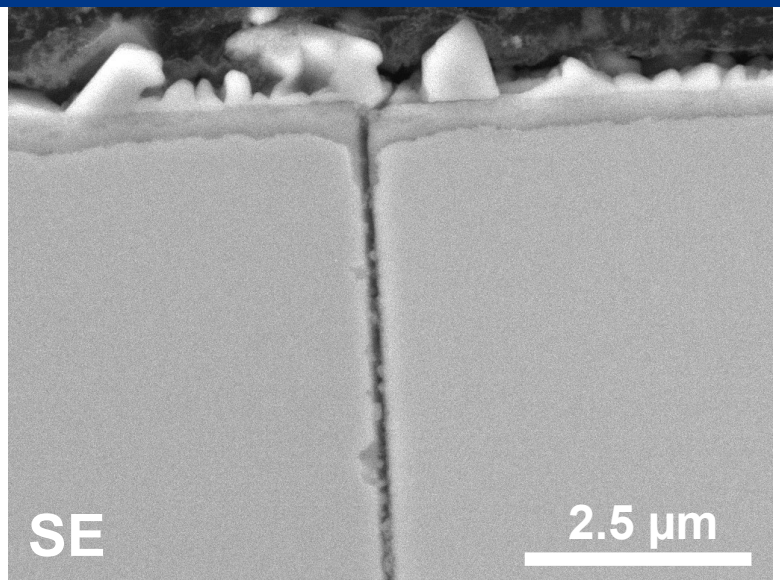

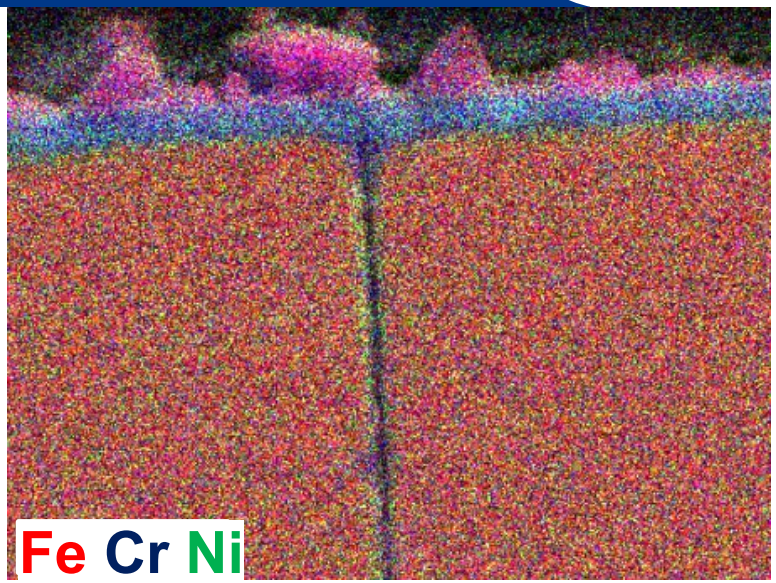

10 kV analyses (X-Max 150 SDD)

- BSE Images: Oxide present on crack walls
- Qualitative oxide EDX SI analysis: extracted elemental maps

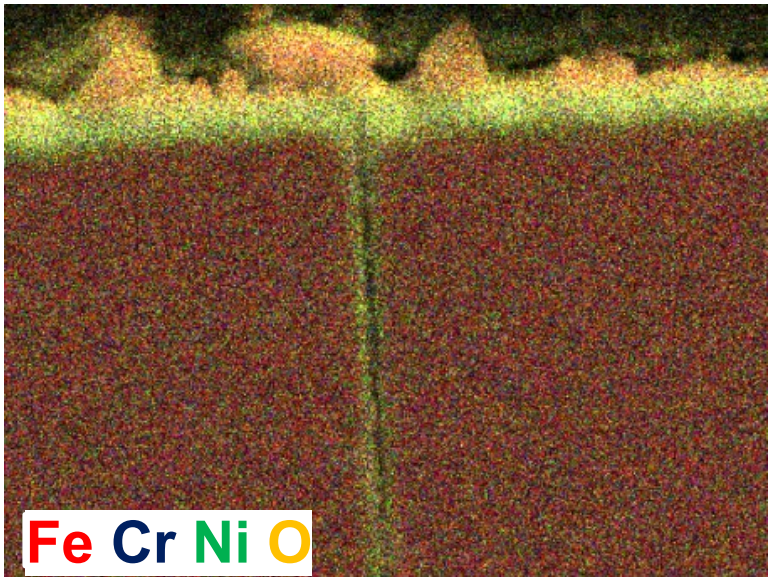

Proton-Irradiated 316L SS: Post-Test Analysis

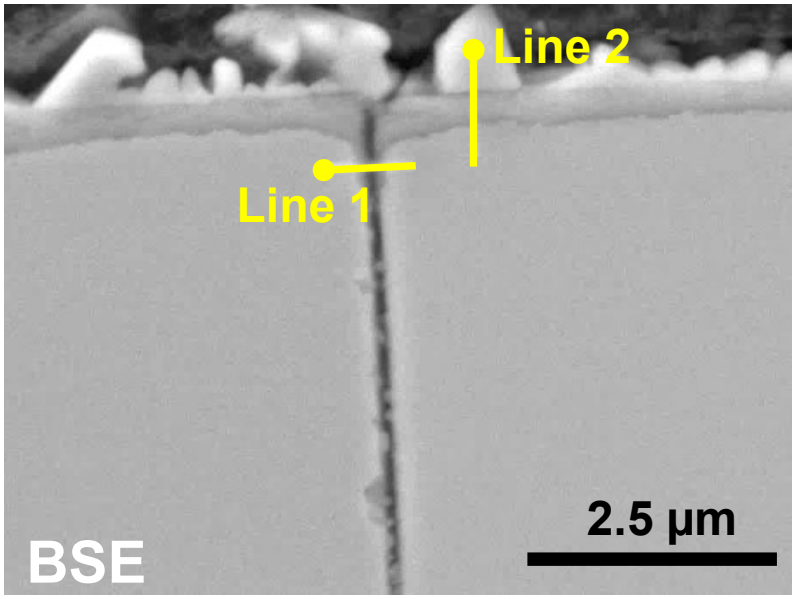

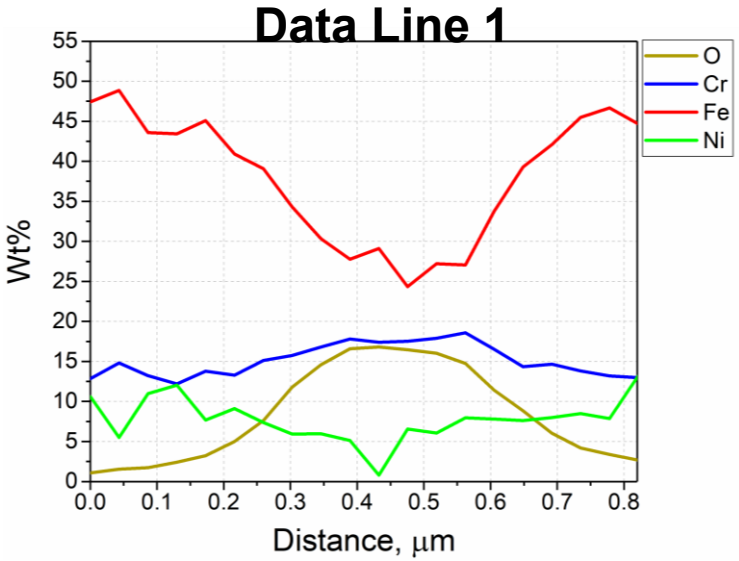

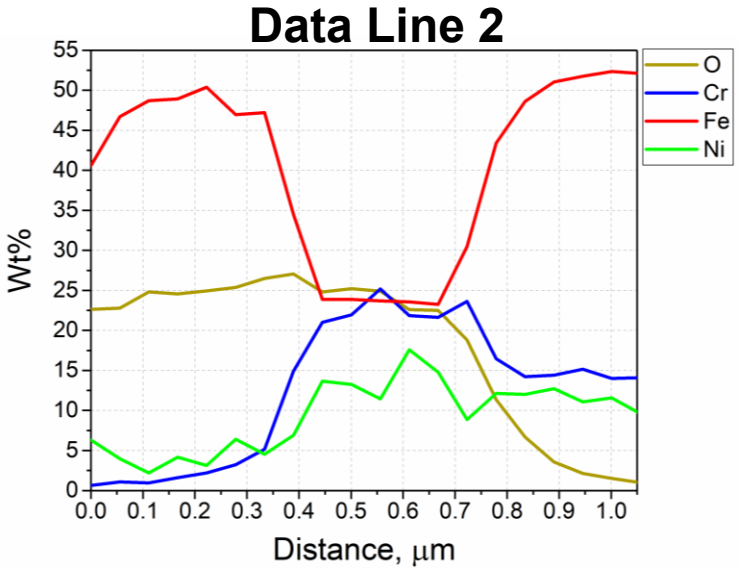

10 kV analyses (X-Max 150 SDD)

- BSE Image: Oxide present on crack walls
- Semi-quantitative profiles

Proton-Irradiated 316L SS: Post-Test Analysis

Summary

Subtask: Post-test Specimen Characterisation

Useful microstructural data can be generated by careful FEGSEM BSE imaging and complementary FEGSEM-EDX Spectrum Imaging and Microanalysis

- BSE image contrast delineation of proton-irradiated region
- Ability to detect oxide variation/Ni enrichments in the vicinity of the SCC oxide-metal interface

Low Voltage EDX SI is capable of 50 nm depth resolution for 3.5 kV accelerating voltage (excellent complement to conventional FEGSEM analyses

And now……. Neutrons!

Task 4.1.3: Characterization of neutron irradiated materials (SEM, TEM)

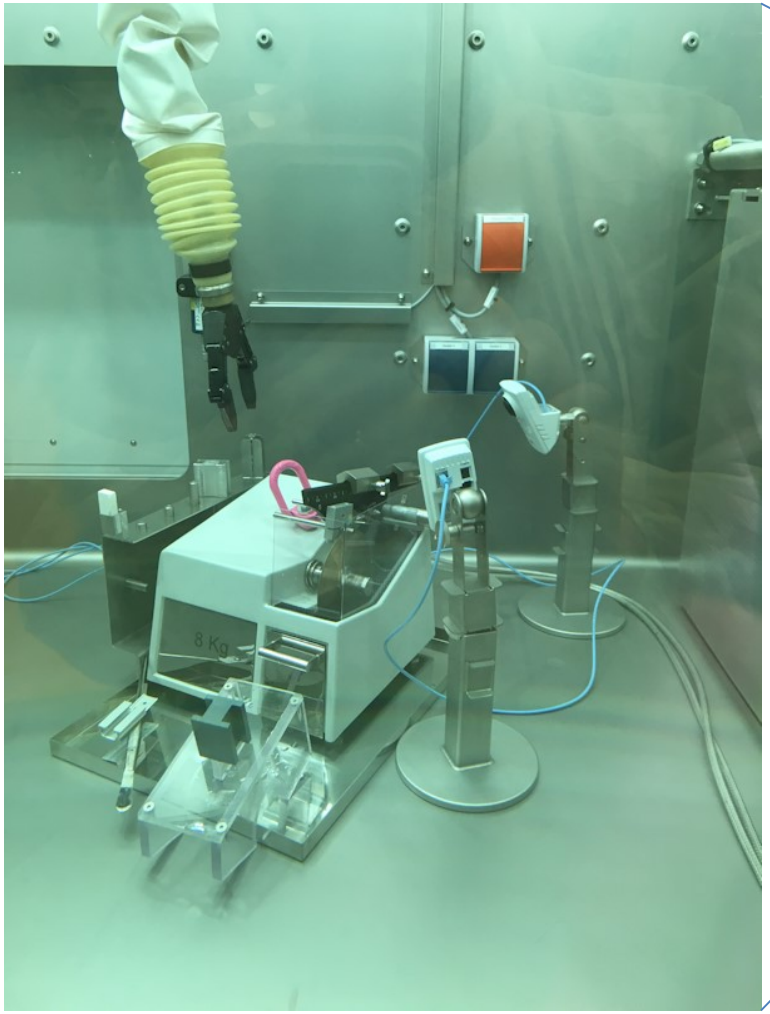

Brief review from Mid-Term Seminar

- Neutron irradiation of metallic materials produces small defect clusters in the matrix, which then serve to harden the material and to make it more prone to localized dislocation glide during plastic deformation
- Particular to irradiated austenitic stainless steels:
  - dislocation channelling
  - stacking fault formation
  - martensite formation
  - deformation twinning

ALL are manifestations of inhomogeneous deformation that can produce band-like features in the deformed microstructure when viewed in TEM.

Brief review from Mid-Term Seminar

0.11 dpa

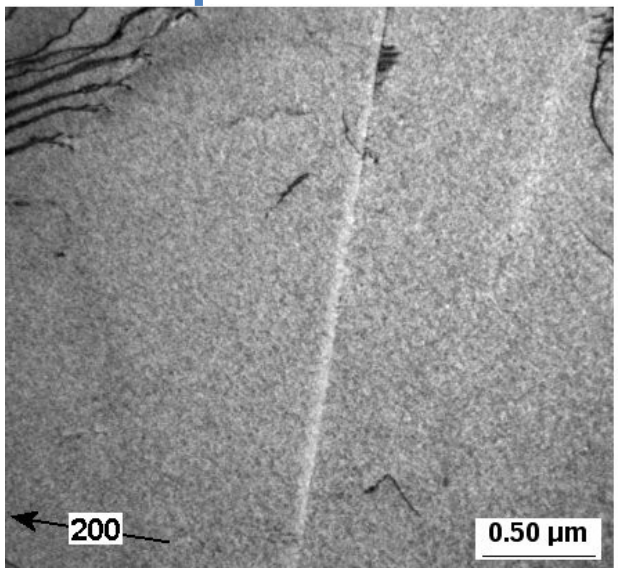

0.16 dpa

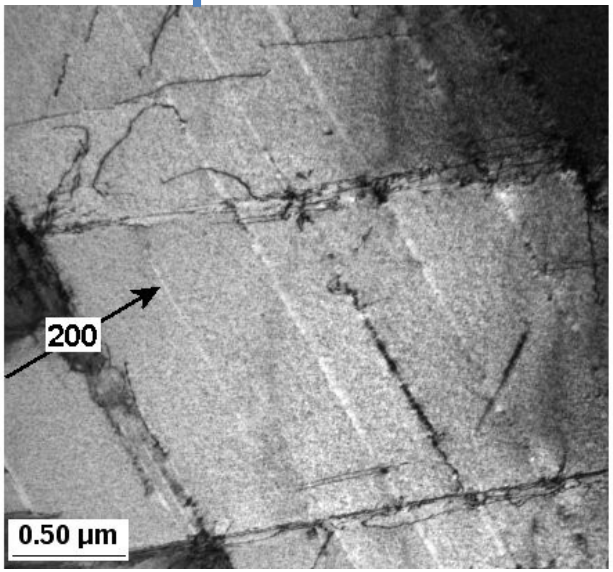

0.89 dpa

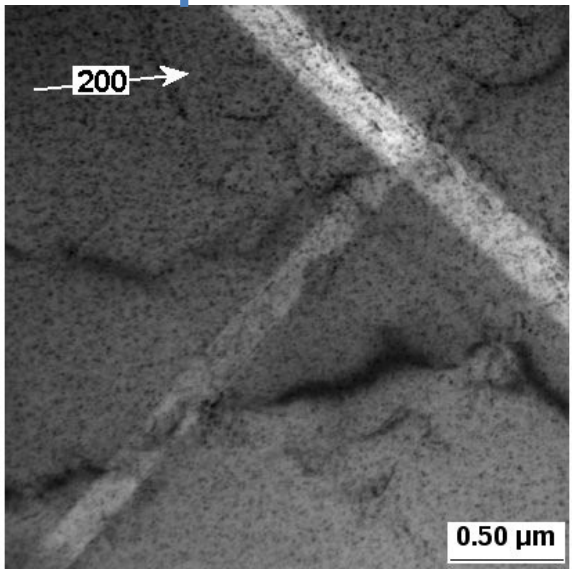

Solution-annealed 304L SS with relatively low amounts of irradiation, followed by low induced strain captures clear-band formation well; localized deformation is important for IASCC.

Brief review from Mid-Term Seminar

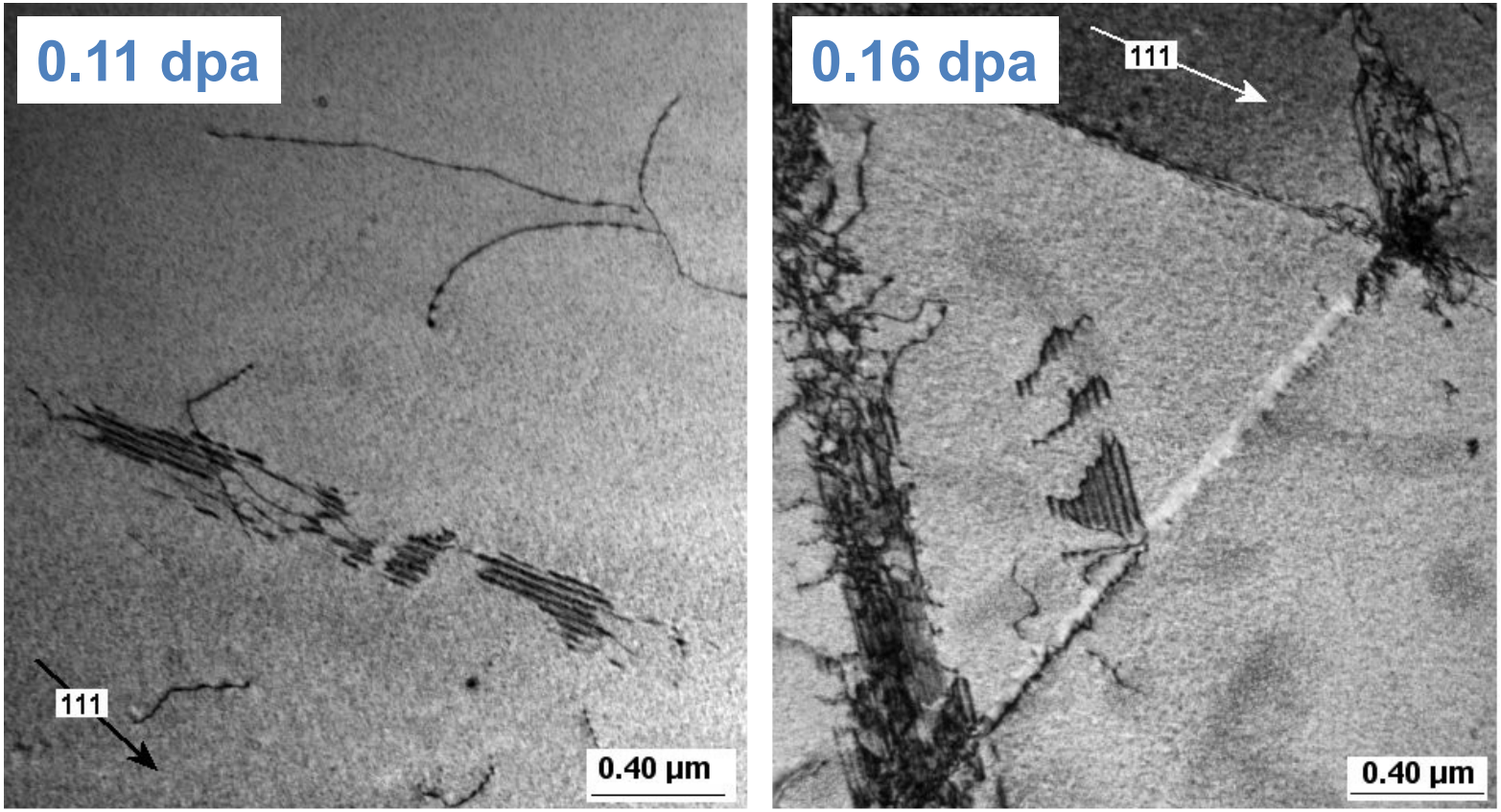

All of the specimens showed stacking faults to some degree as well, generally restricted to the channels.

Brief review from Mid-Term Seminar

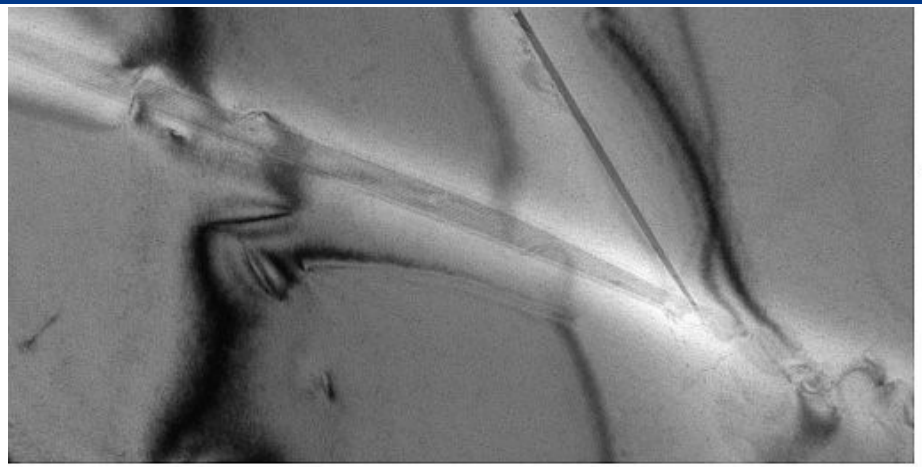

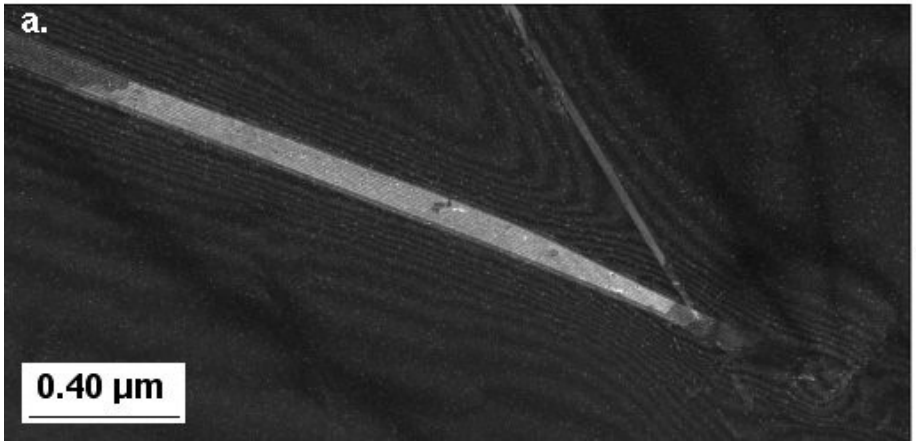

0.11 dpa

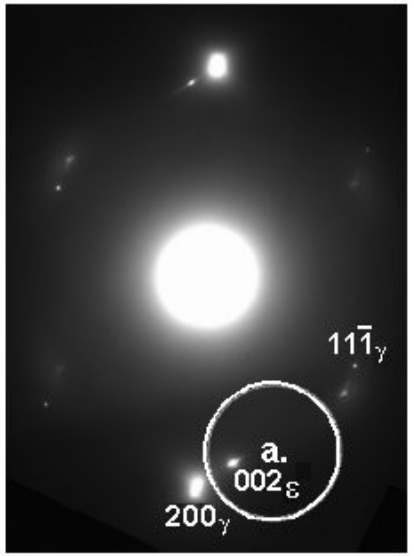

Upon accumulation of several stacking faults, satellite spots have distinct d-spacing which correspond most closely to that of HCP-epsilon martensite.

Brief review from Mid-Term Seminar

0.16 dpa

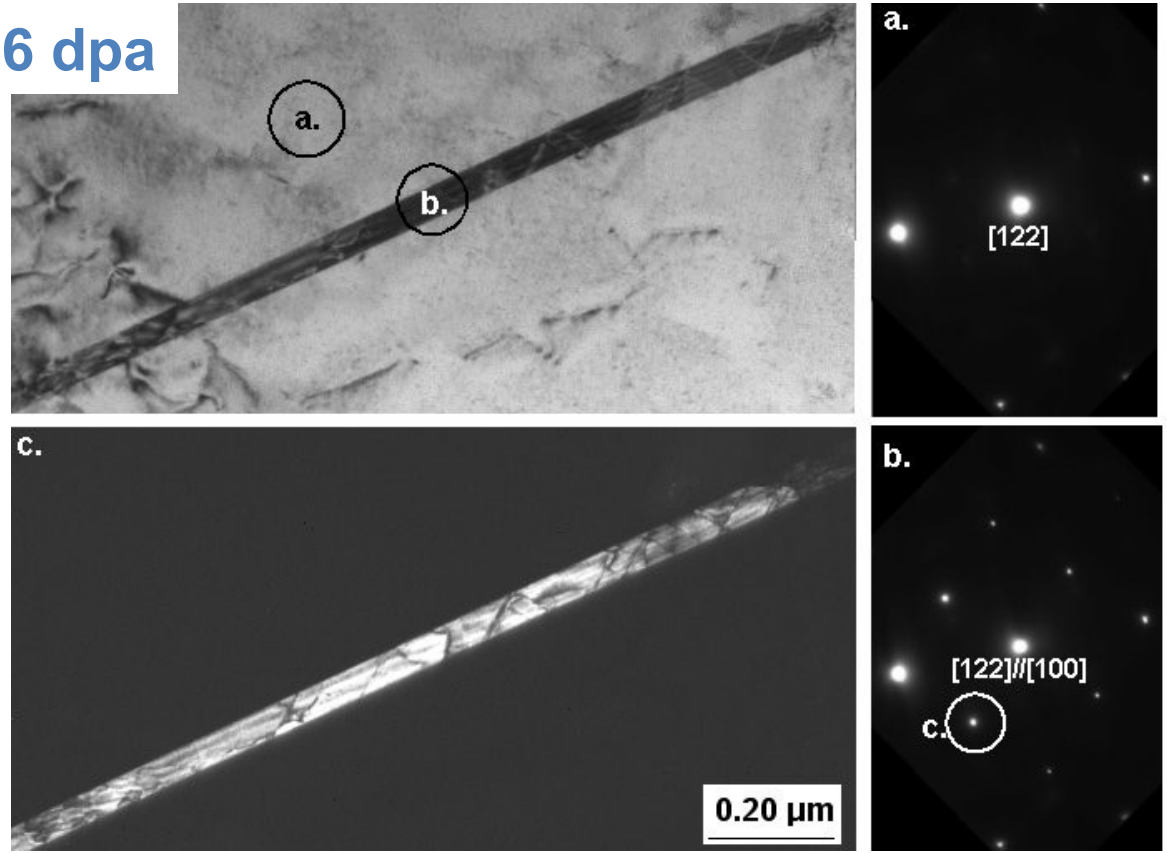

Further accumulation of overlapping stacking faults in a band introduced strong reflections corresponding to austenite phase of different orientation, indicating the formation of a twin.

Brief review from Mid-Term Seminar

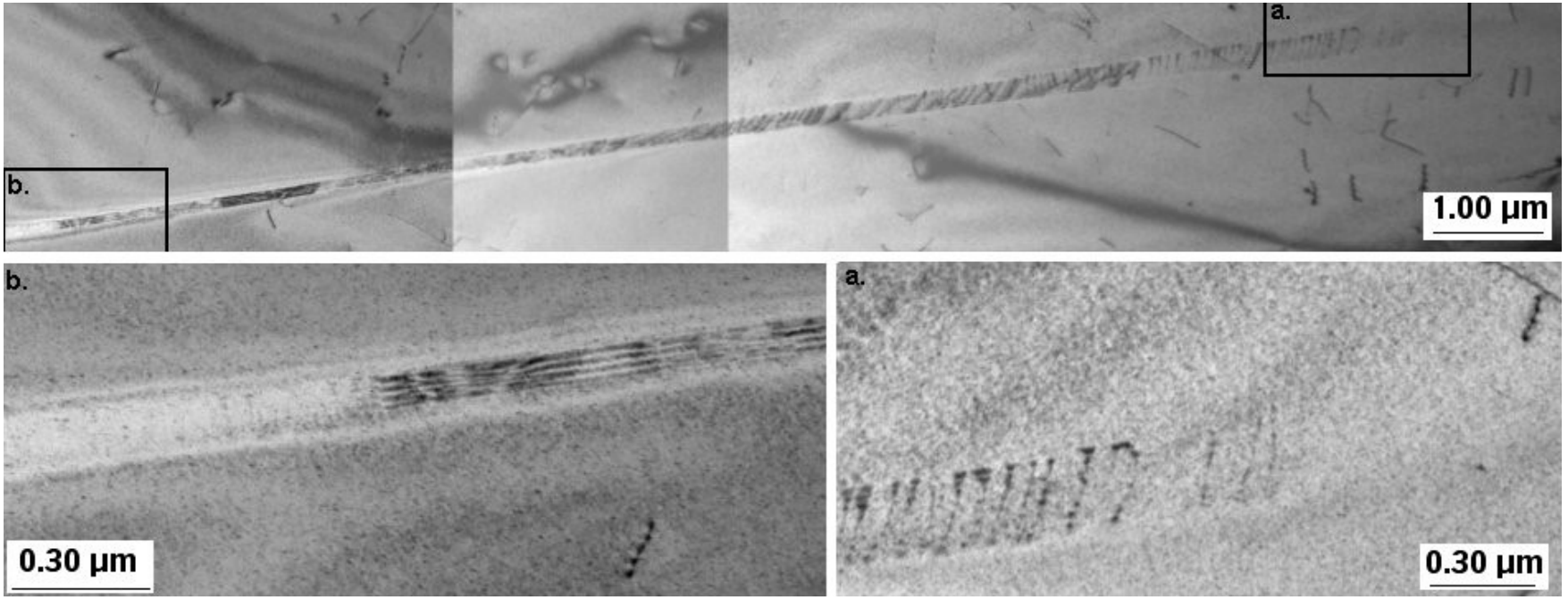

Channel in 0.11 dpa material demonstrates several stages of evolution process:

- head of channel marked by several dislocations (a.)
- followed by gradual separation of partial dislocations, overlapped in some regions → strong contrasts indicating different planar stacking
- left behind a band with reduced defect density (b.).

Irradiation effects on increasing dpa

In cold-worked 304 SS material, radiation annihilates linear dislocations and replaces with dislocation loops.

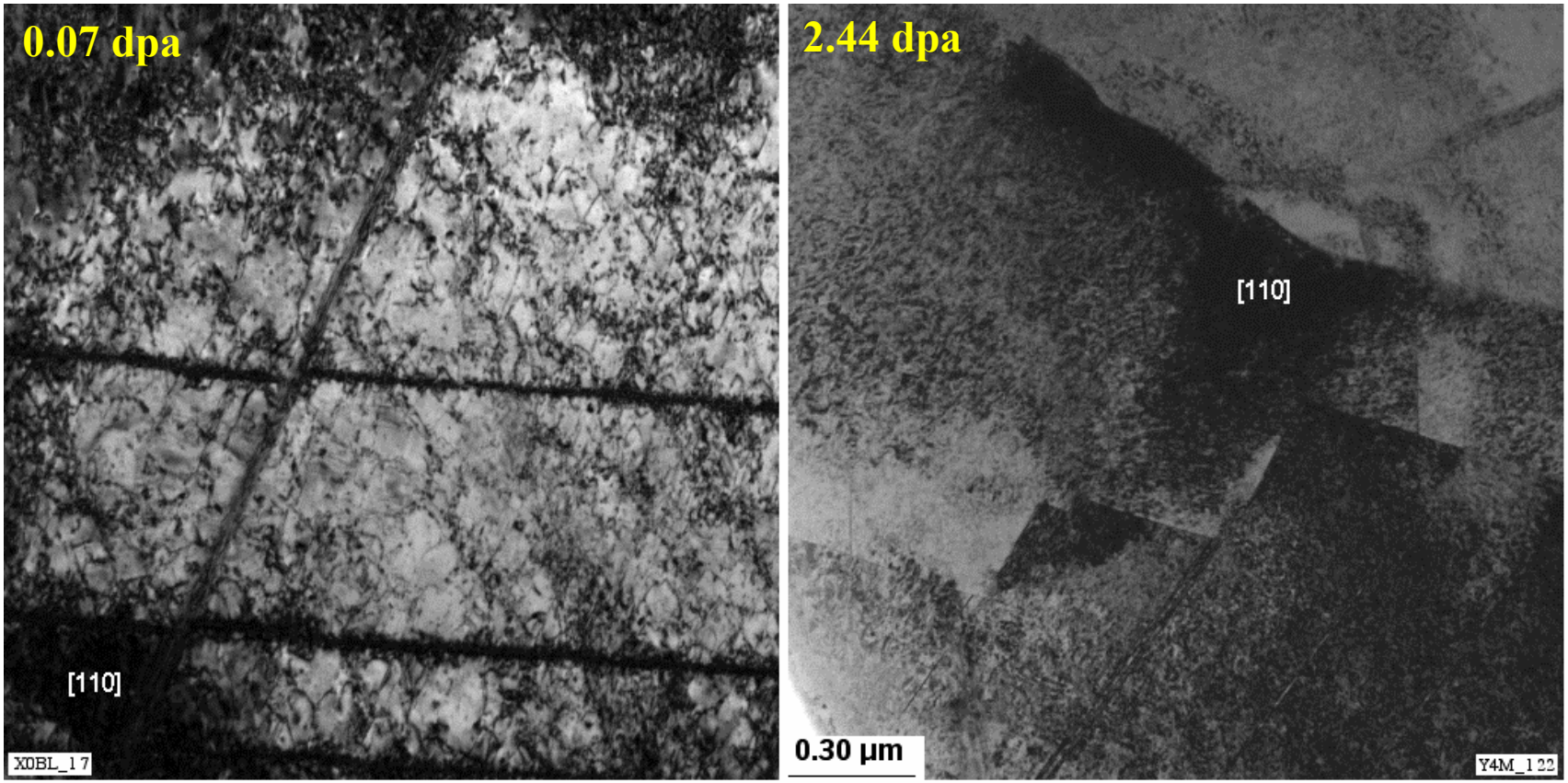

Results from EU-PERFECT project

Irradiation effects on increasing dpa

In cold-worked 304 SS material, radiation annihilates linear dislocations and replaces with dislocation loops.

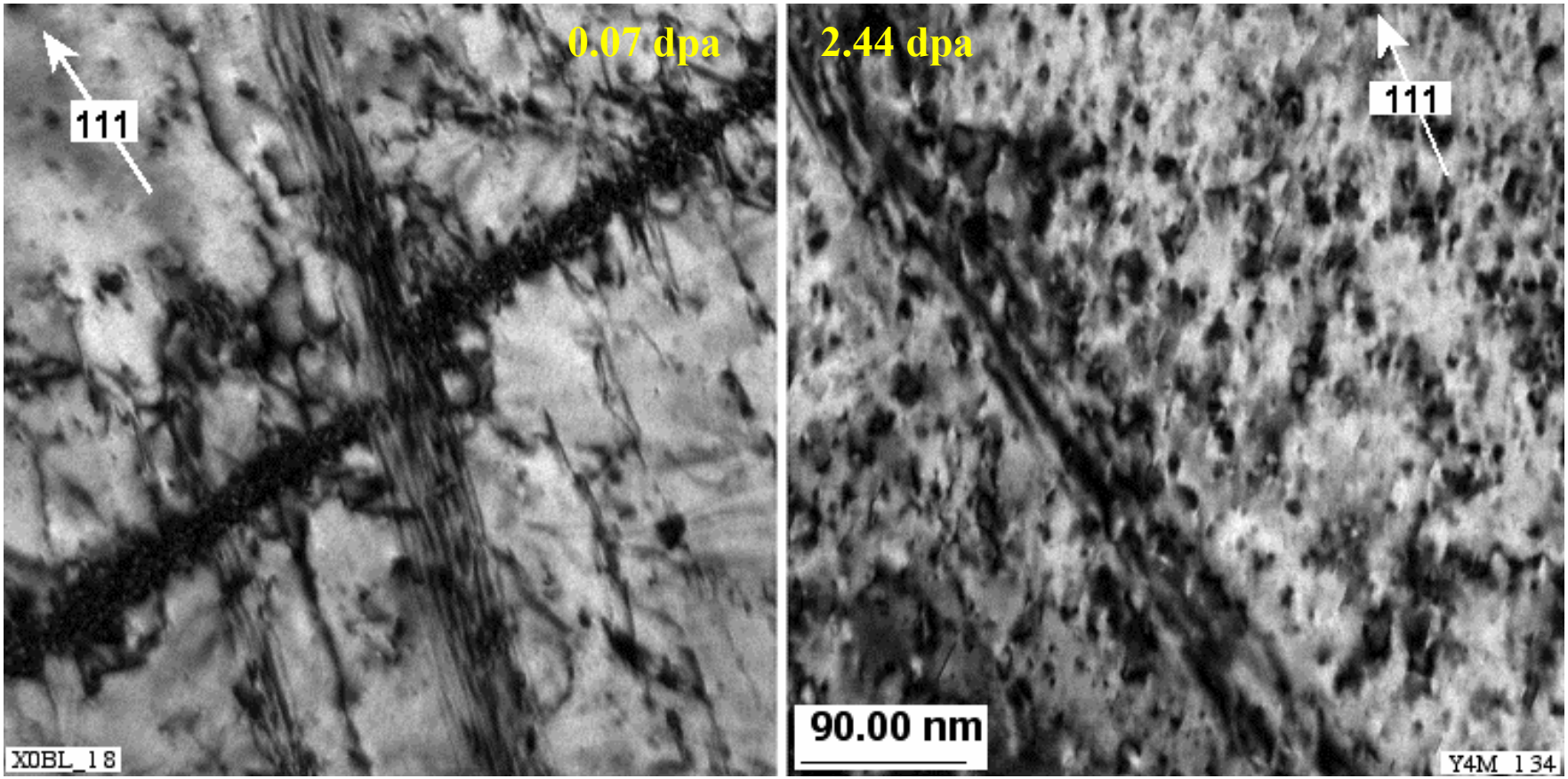

Results from EU-PERFECT project

Irradiation effects on increasing dpa

Faulted dislocation loop population is typically viewed and quantified by employing rel-rod dark-field method.

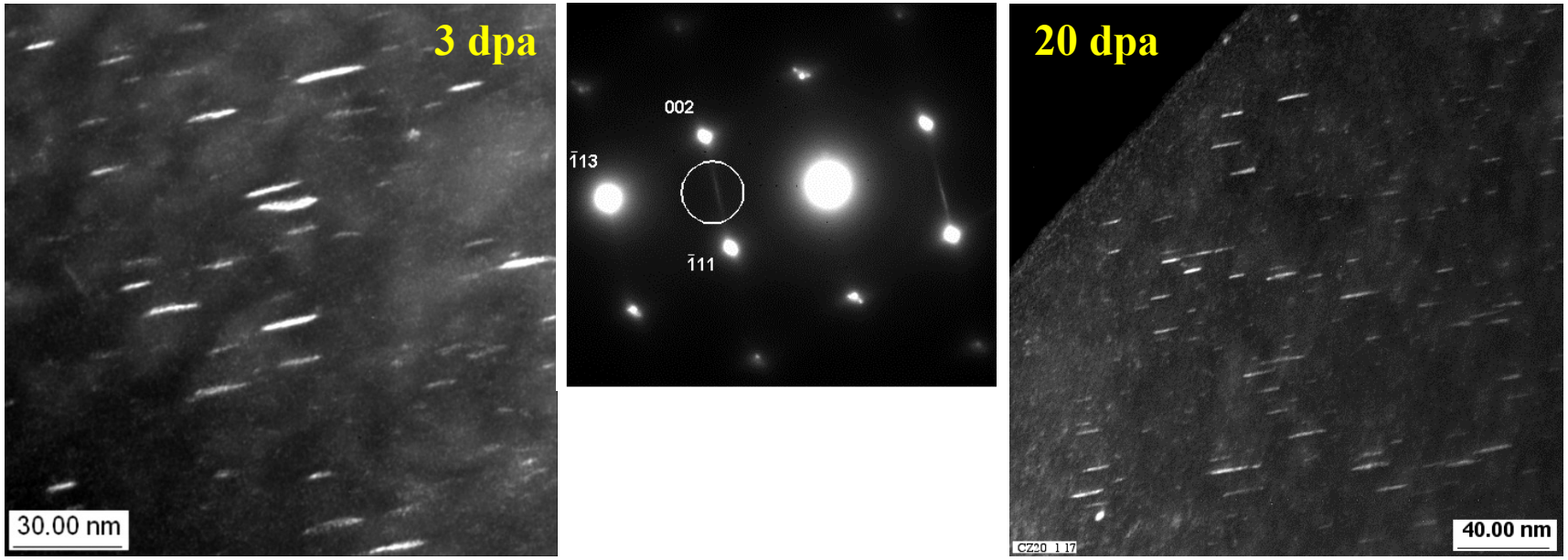

Power-reactor irradiated solution annealed 304 SS

Irradiation effects on increasing dpa

At very high dpa's, precipitation of a Ni&Si-rich phase emerges in the matrix (gamma prime).

- Coherence with matrix is evident from SAD pattern, and also by Moiré contrasts in BF image, but DF-imaging is still possible.

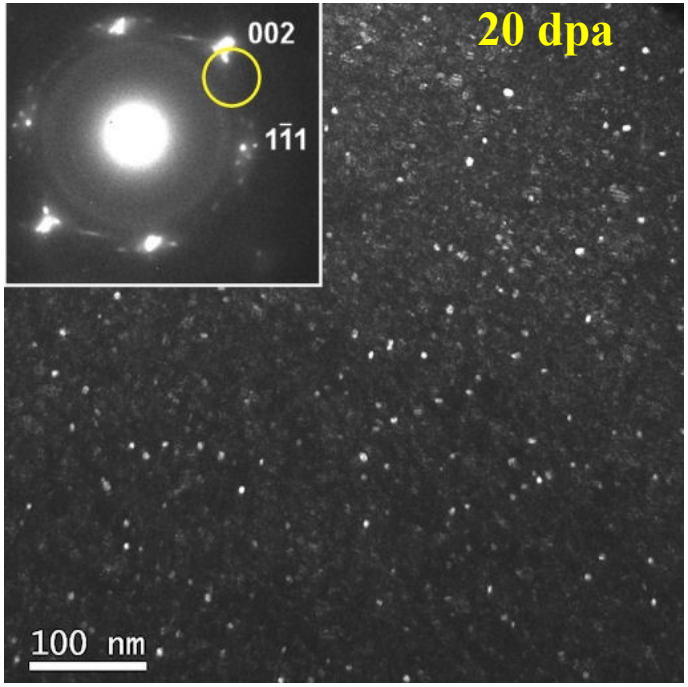

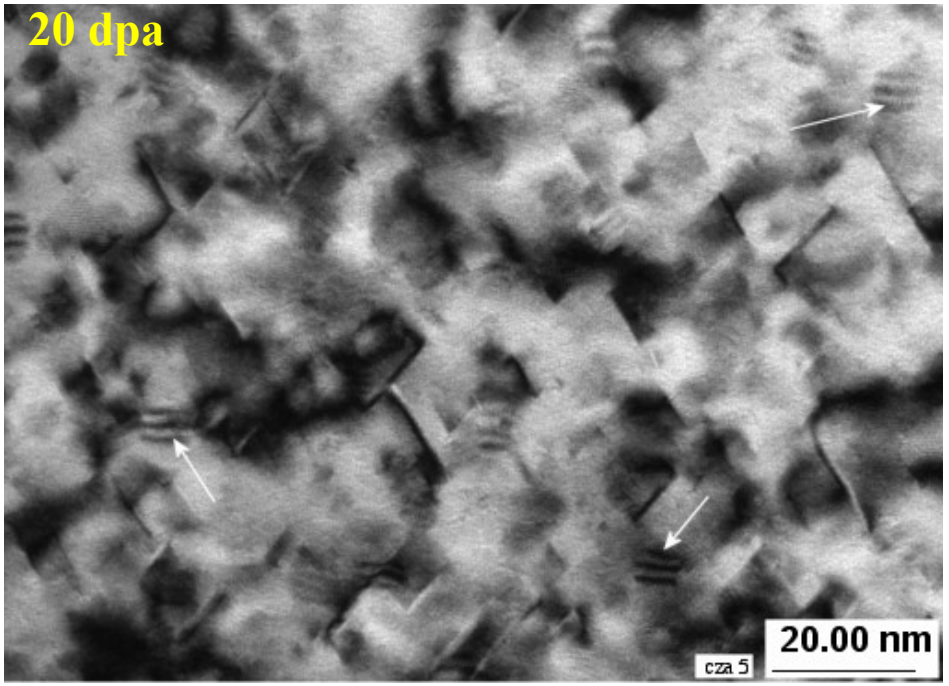

Power-reactor irradiated solution annealed 304 SS

Irradiation effects on increasing dpa

Grain boundaries experience increasing radiation-induced segregation with increased dpa.

- Significant Ni- and Si-enrichments; **Fe** and Cr-depletion

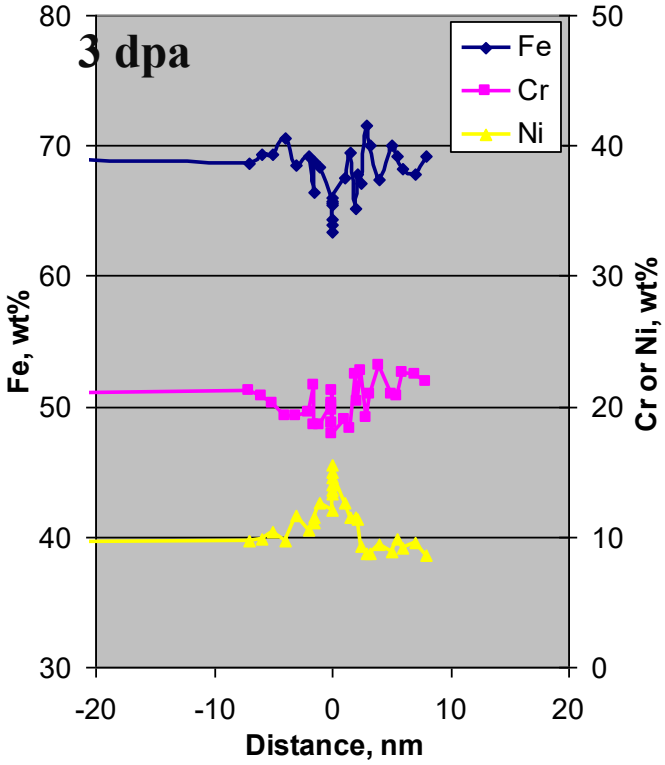

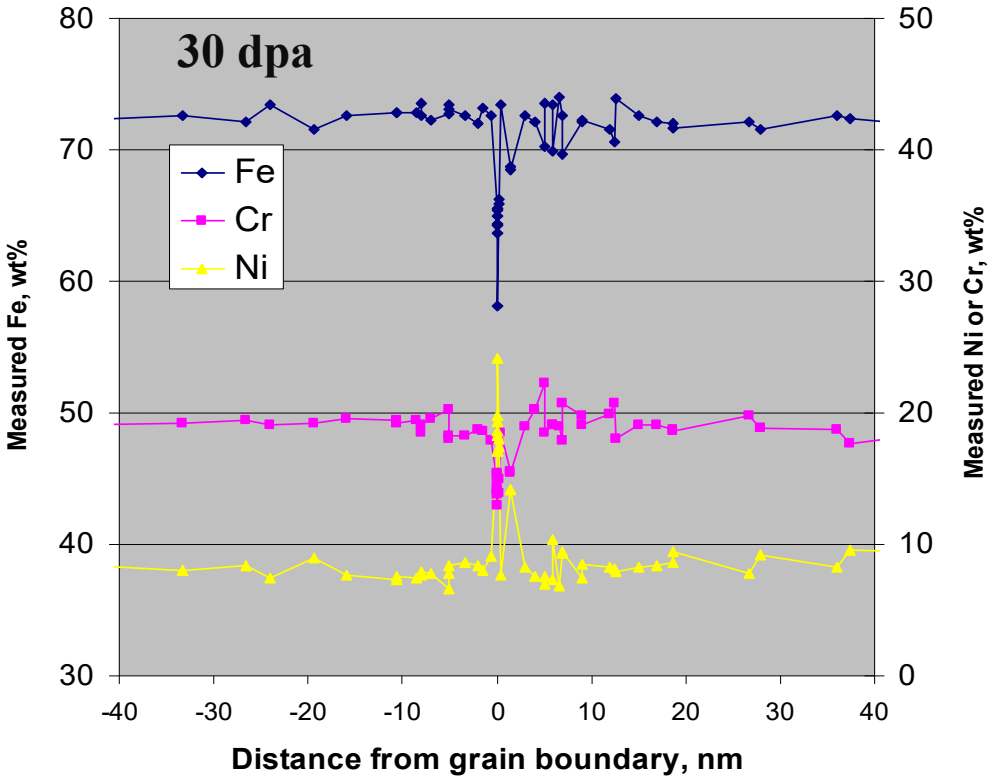

Irradiation effects on increasing dpa

- RIS at GBs and as precipitates in 30 dpa SA 304L.

Magnitude of fluctuation at grain boundary

Location	Fe	Cr	Ni	Si
At GB	-12.1	-7.6	15.8	4.03
5 nm from GB	1.4	3.0	-3.8	-0.7

Matrix precipitate composition

Precipitate	Fe	Cr	Ni	Si
1	36.1	7.6	50.1	6.25
2	52.6	12.0	30.1	5.32
3	47.2	9.6	36.5	6.77
4	55.4	14.5	26.6	3.47
5	61.2	13.5	22.1	3.16

Adjacent the precipitates a few wt% Ni depletion,Cr enrichment

W. Karlsen et al., HPR-369 Vol. 2, Enlarged Halden Group Meeting, 2008

Irradiation effects on increasing dpa

At very high dpa's, cavities also emerge in the matrix.

- Viewed at high magnification in slightly under-focus condition.
- Size of cavities may be more thermally-dependent than dpa-dependent, as different components (locations in reactor) exhibit different cavity populations.

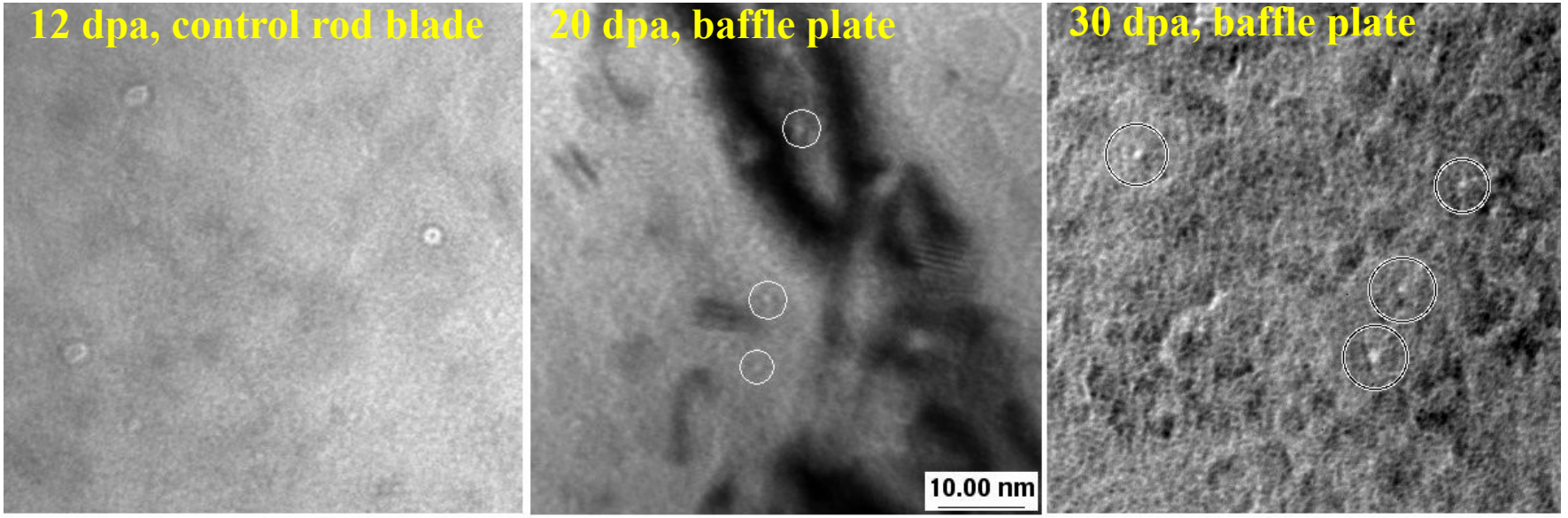

Power-reactor irradiated solution annealed 304 SS

Irradiated baffle bolt at 17 dpa area

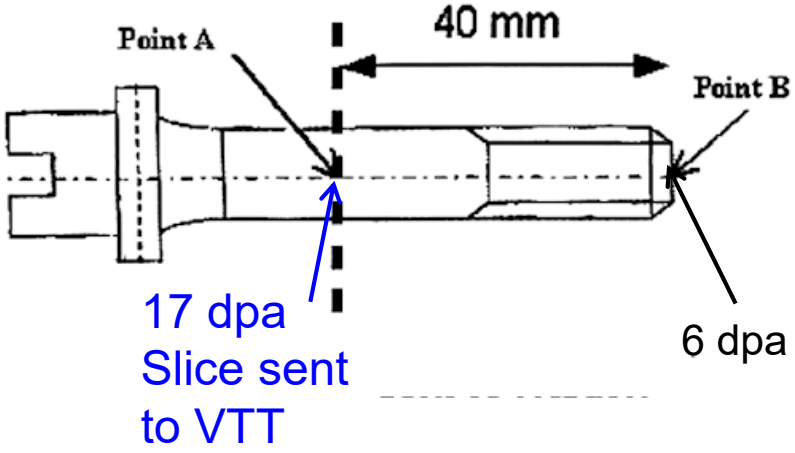

19 operation cycles at
350 – 390 °C (in middle of bolt.)

Halden IASCC Review Meeting
17-18 October 2012, Halden
Wade Karlsen and Janne Pakarinen

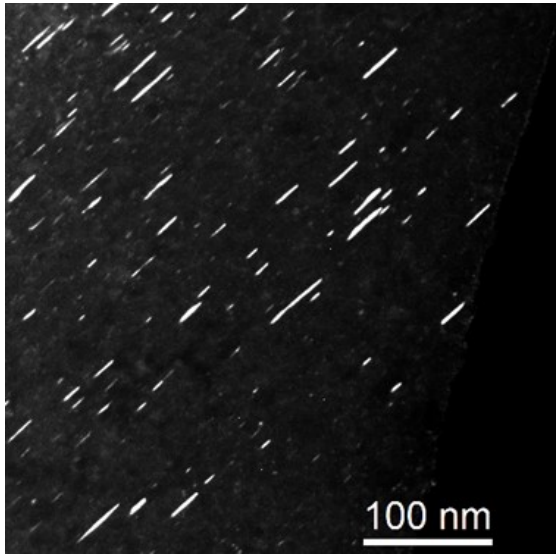

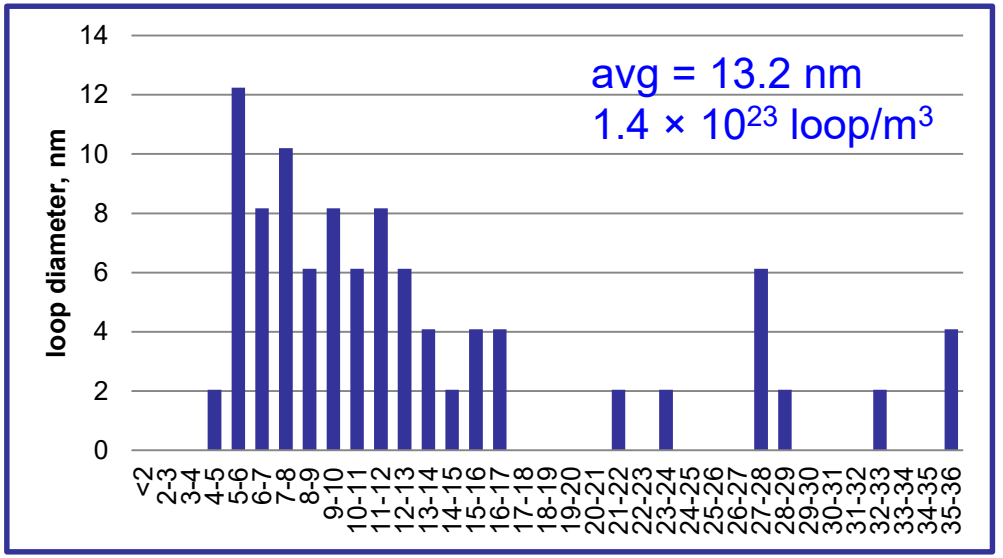

Irradiated baffle bolt at 17 dpa area

- Analysis of radiation-induced segregation

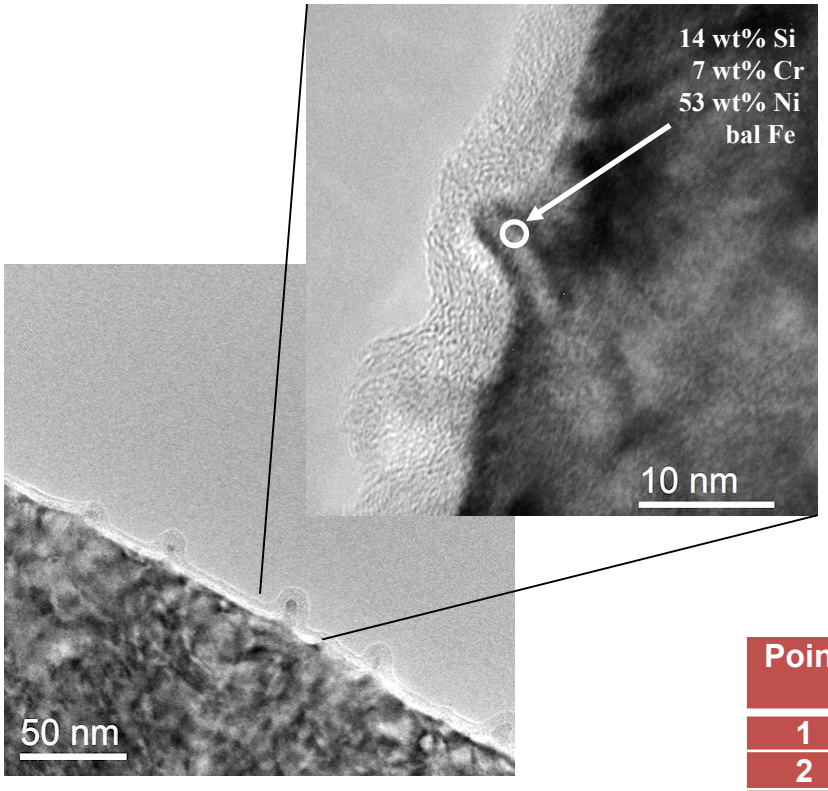

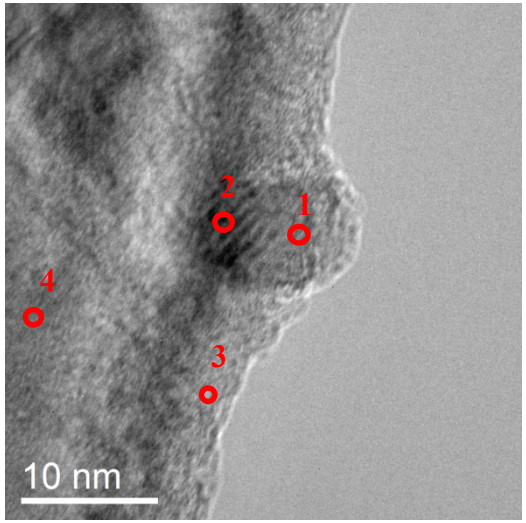

Point	Si (wt%)	Cr (wt%)	Ni (wt%)	Mo (wt%)	Fe
1	12.6	8.0	44.0	1.5	bal
2	2.9	16.0	21.8	2.5	bal
3	0.7	24.9	8.3	4.8	bal
4	0.8	21.0	10.4	3.2	bal

Halden IASCC Review Meeting
17-18 October 2012, Halden
Wade Karlsen and Janne Pakarinen

Note that Fe is depleted when Cr is depleted

Irradiated baffle bolt at 17 dpa area

- Analysis of radiation-induced segregation

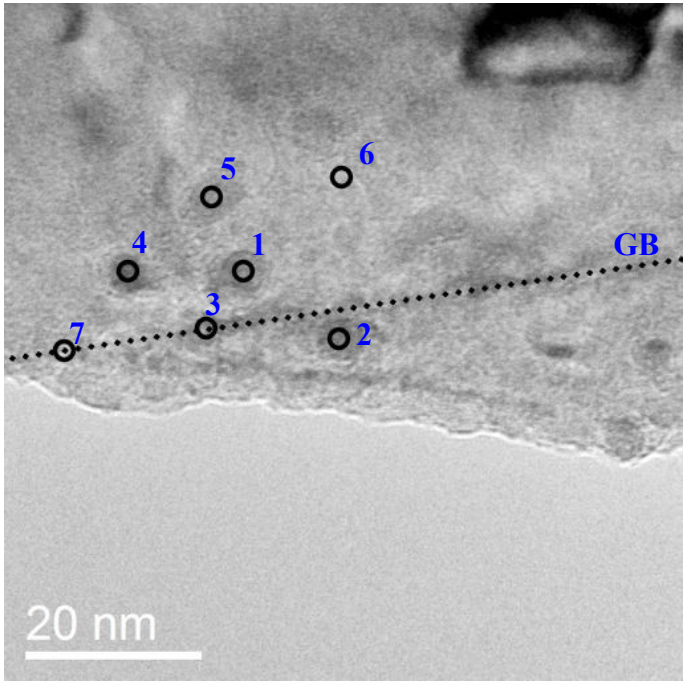

Grain boundary composition

	Si (wt%)	Cr (wt%)	Ni (wt%)	Mo (wt%)	Fe
All (Ni wt% >20)	4.7 ± 0.9	14.8 ± 0.9	21.9 ± 1.1	2.2 ± 0.5	bal
Max	6.3	13.9	23.4	2.7	bal

Point analyses in vicinity of GB

Point	Si (wt%)	Cr (wt%)	Ni (wt%)	Mo (wt%)	Fe
1	7.3	13.3	27.8	1.6	bal
2	4.8	15.2	20.5	2.2	bal
3	4.0	13.5	15.6	1.3	bal
4	5.8	15.0	18.6	1.0	bal
5	4.2	19.1	20.9	2.7	bal
6	1.3	20.3	12.8	3.9	bal
7	12.9	10.3	42.1	0.7	bal

Halden IASCC Review Meeting
17-18 October 2012, Halden
Wade Karlsen and Janne Pakarinen

Irradiated baffle bolt at 17 dpa area

- Analysis of radiation-induced segregation

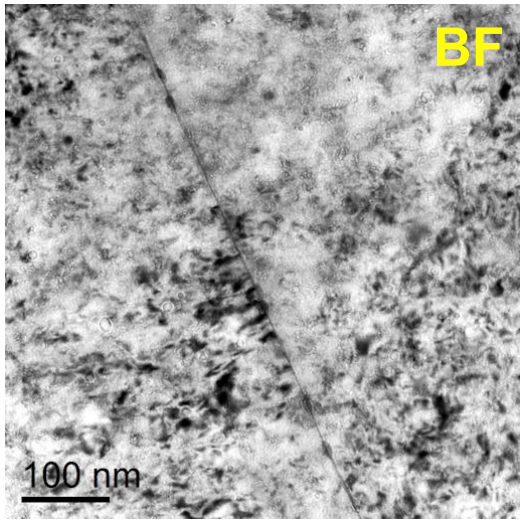

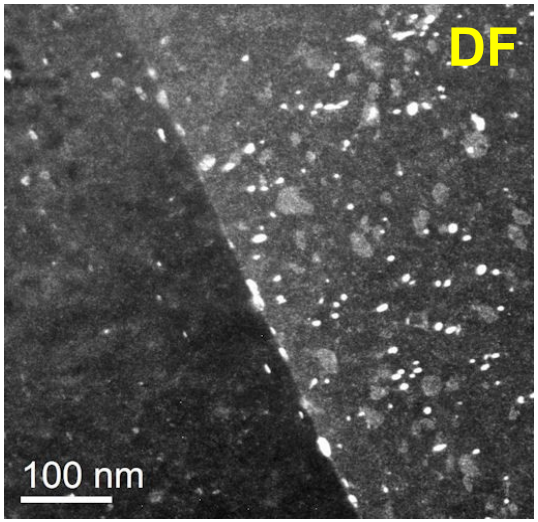

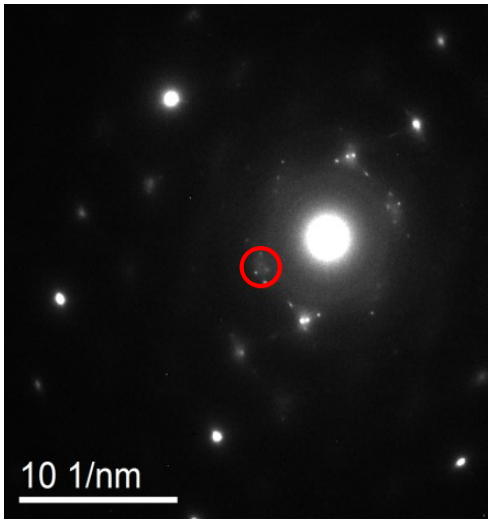

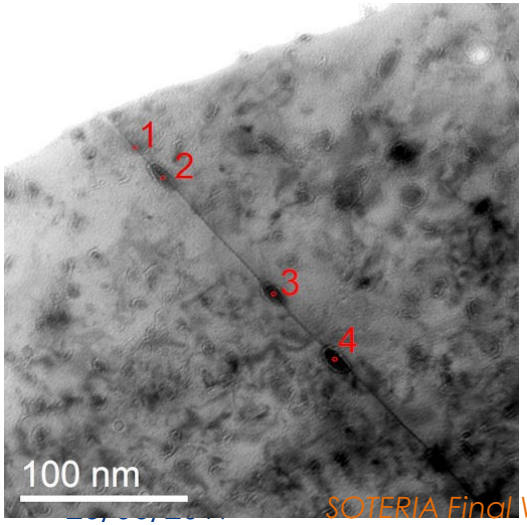

Halden IASCC Review Meeting
17-18 October 2012, Halden
Wade Karlsen and Janne Pakarinen

Point	Si (wt%)	Cr (wt%)	Ni (wt%)	Mo (wt%)	Fe
1	5.0	14.9	22.3	1.8	bal
2	10.5	11.6	36.7	1.6	bal
3	11.7	12.9	42.0	1.7	bal
4	8.6	13.8	26.3	1.3	bal

Irradiated baffle bolt at 17 dpa area

- Analysis of cavities and cavity-RIS

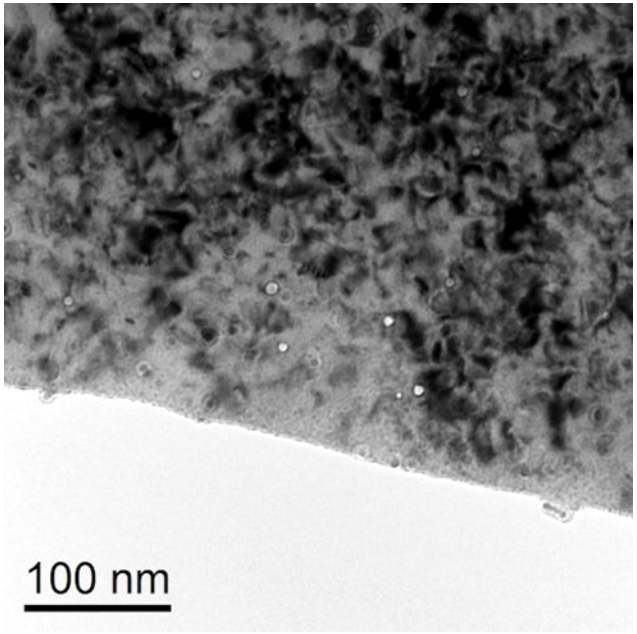

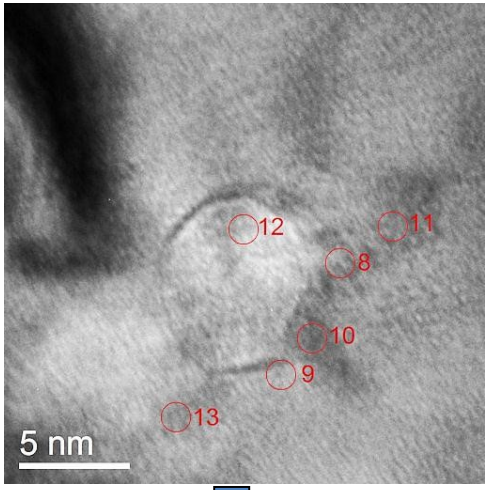

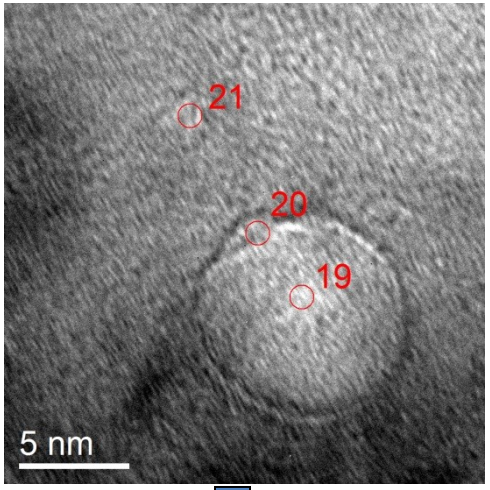

Point	Si (wt%)	Cr (wt%)	Ni (wt%)	Mo (wt%)	Fe
8	6.5	12.1	31.2	0.7	bal
9	1.2	18.3	12.6	3.0	bal
10	1.6	16.4	15.7	3.0	bal
11	2.6	16.7	18.6	3.1	bal
12	2.0	17.6	13.6	1.8	bal
13	1.1	18.2	12.9	2.0	bal
19	1.2	19.2	13.0	1.8	bal
20	1.3	19.0	13.7	2.5	bal
21	0.5	20.8	8.5	1.6	bal

Halden IASCC Review Meeting
17-18 October 2012, Halden
Wade Karlsen and Janne Pakarinen

Irradiated baffle bolt at 17 dpa area

- Analysis of cavities and cavity-RIS
  - Bright field/dark field image pair of one void region reveals a precipitate associated with the void.
  - SAD of the examined region showed the presence of precipitates with a lattice relation to the matrix (small spots).
  - Voids shrank upon EDS analysis.

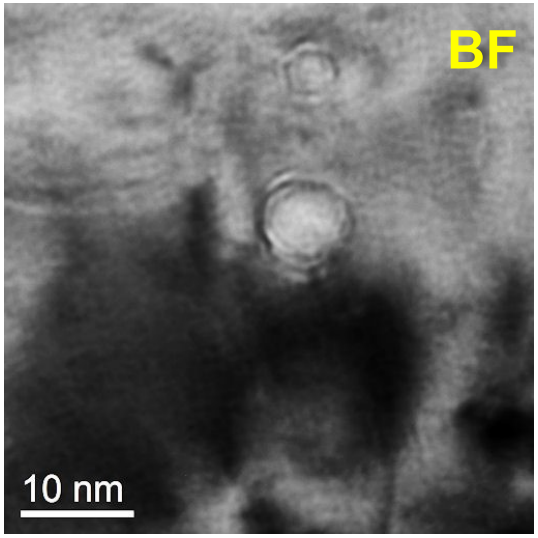

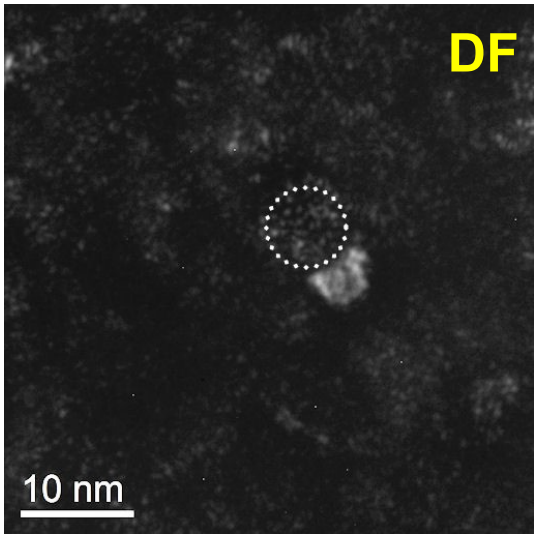

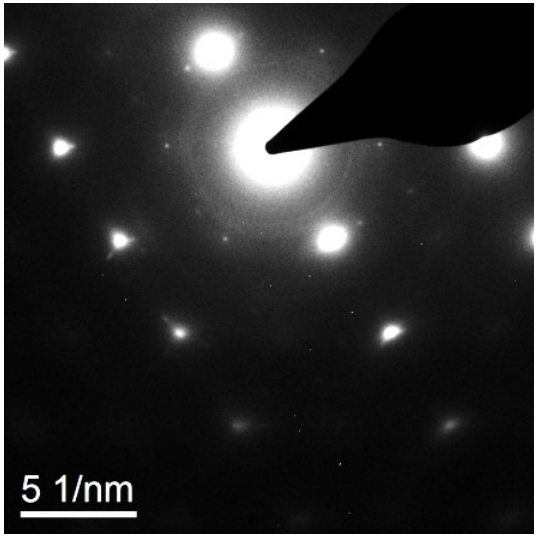

Halden IASCC Review Meeting
17-18 October 2012, Halden
Wade Karlsen and Janne Pakarinen

Irradiated baffle bolt at 17 dpa area

- Summary of observations from 17dpa baffle bolt slice
  - Frank loops with a concentration of 1.4×10^{23} loop/m^3 were found. Average loop size was 13.2 nm.
  - GBs showed clear RIS, as well as the presence of precipitates rich in Si and Ni.
  - One ppt phase was identified as γ' (Ni_3Si); had a lattice relation with fcc matrix.
  - Voids/bubbles ~5-10 nm were present in the microstructure.
  - Void walls also showed clear RIS. However, there were indications that the RIS was not constant at the void surfaces.
  - Voids and precipitates were found to often be associated with one another.
  - Voids shrank upon EDS analysis, which could indicate either gas diffusion out of them, or flux of interstitials to the void wall.

Halden IASCC Review Meeting
17-18 October 2012, Halden
Wade Karlsen and Janne Pakarinen

IASCC deformation and fracture

- At PWR operating temperatures, irradiated stainless steels ruptured by tension in air, or in argon, generally display dimpled-ductile (transgranular) fracture
- IG fractures have *also* been reported for irradiated austenitic stainless steels subjected to **slow strain rate** testing, including in inert environment
- IG fracture is also known to take place under impact loading conditions for specimens charged with hydrogen

Prediction of instances and extent of cracking could enable better assessment of the integrity of reactor structural components

IASCC example study

- VTT has tested and examined a 304 stainless steel that had been removed from service in an actual nuclear reactor.
- Material was taken from a region having accrued a dose of 30 dpa, or $2 \cdot 10^{22}$ n/cm^2 (E>1 MeV) at T_{irr} of ~300°C.
- Noteworthy is that the Si content is slightly higher than typical for modern nuclear grades (e.g. ASTM SA-240, which limits Si to <0.75wt%).

SA 304 SS composition (wt.%) of reference study; balance Fe

C	Si	Mn	S	Mo	Cu	Ni	Cr	P	Co	N
0.060	0.78	0.96	0.003	0.02	0.09	9.3	18.6	0.011	0.034	--

IASCC example study; loading

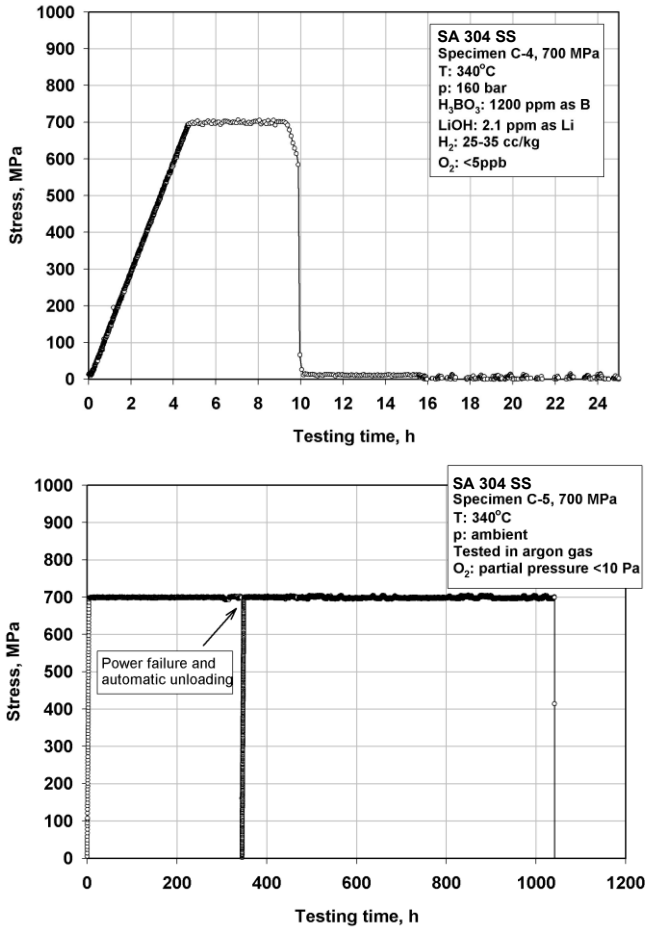

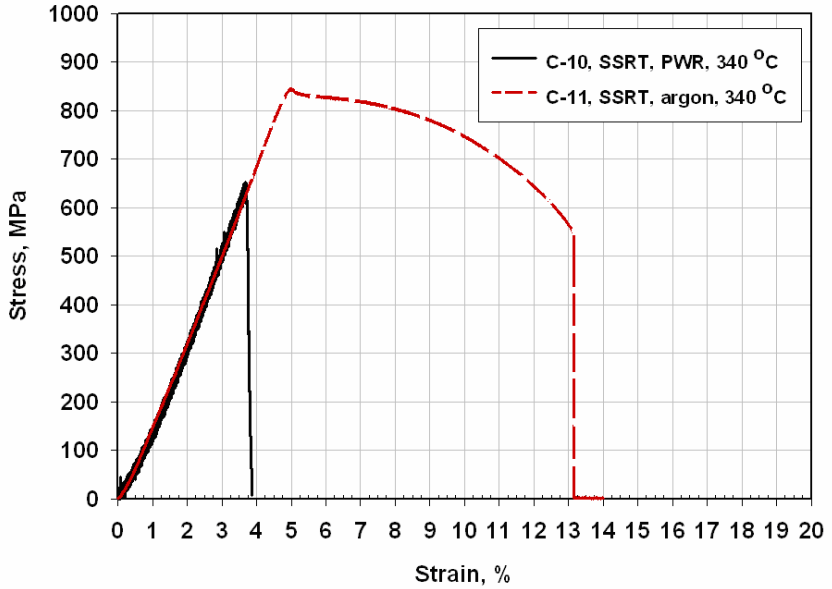

Specimen	Test type*	Environment**
C-4	CL, 700 MPa	PWR, 340 ˚C
C-5	CL, 700 MPa	Argon, 340 ˚C
C-10	SSRT, 10^{-7} s^{-1}	PWR, 340 ˚C
C-11	SSRT, 10^{-7} s^{-1}	Argon, 340 ˚C

*CL = Constant Load test; SSRT = Slow Strain Rate Tensile test.
**PWR=1200 ppm B added as H_3BO_3, 2.1 ppm Li added as LiOH and 30 cc/kg H2.

IASCC example study; fractures

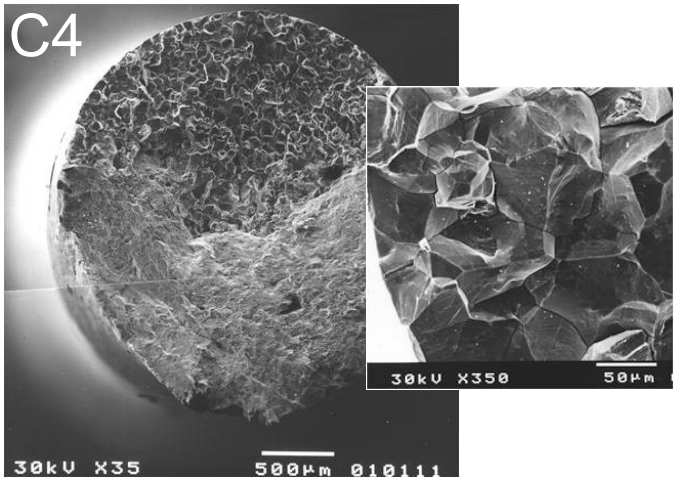

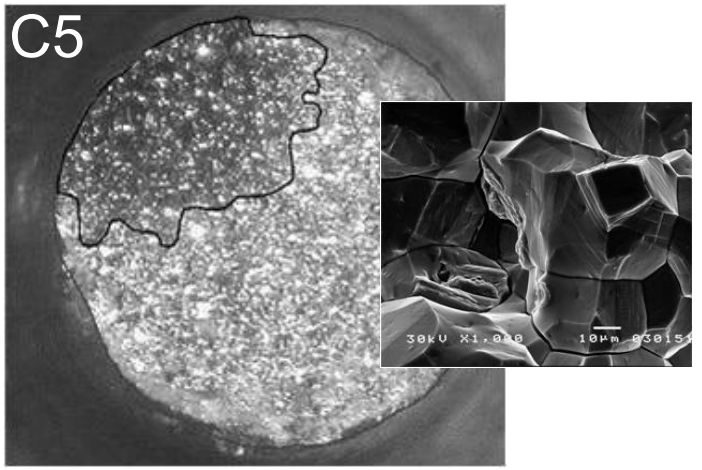

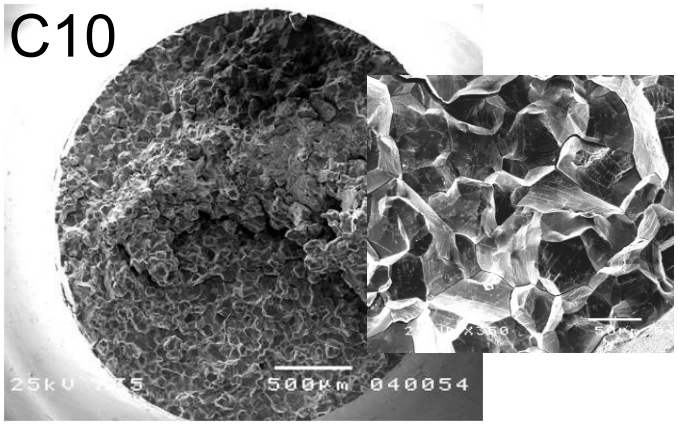

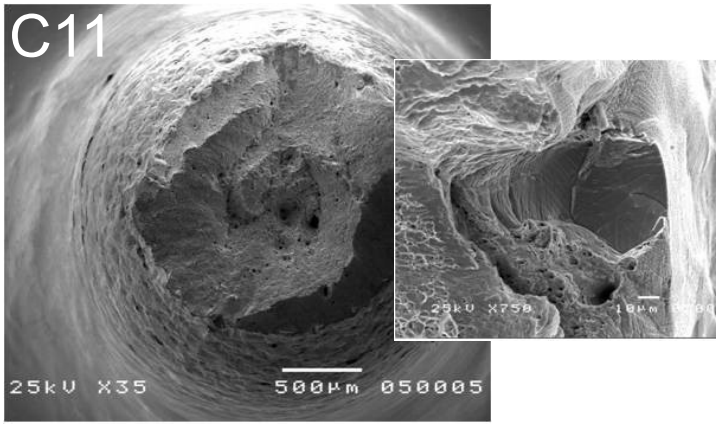

IASCC example study; TEM sampling

TEM specimen	Test bar	Distance from fracture
C4_2	C4 (CL)	1.5 mm
C5_1	C5 (CL)	0.5 mm
C5_2	C5 (CL)	2.0 mm
C10_1	C10 (SSRT)	0.5 mm
C11_2	C11 (SSRT)	1.0 mm
C11_3	C11 (SSRT)	1.5 mm
C11_5	C11 (SSRT)	2.0 mm
C11_5	C11 (SSRT)	~ 15 mm

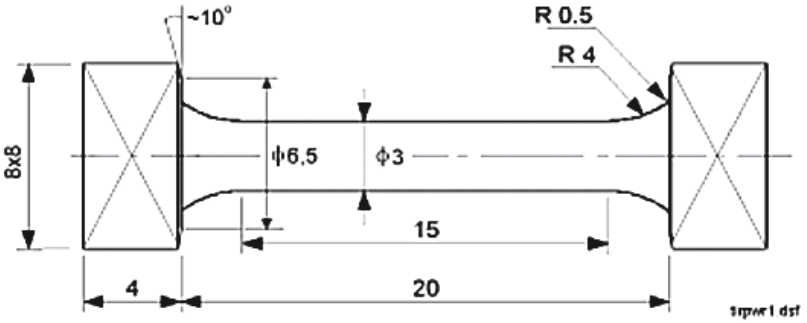

EU-PERFORM60 project (Grant Agreement: 232612)

IASCC example study; deformation

C11

Argon, 340 ˚C
1 mm from FS

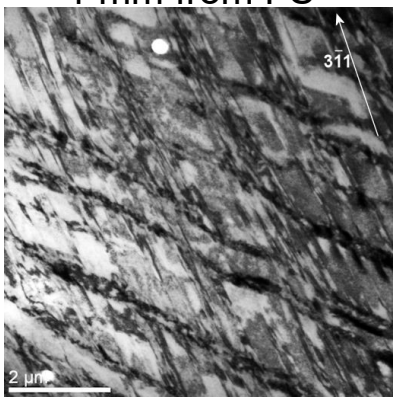

Argon, 340 ˚C
1.5 mm from FS

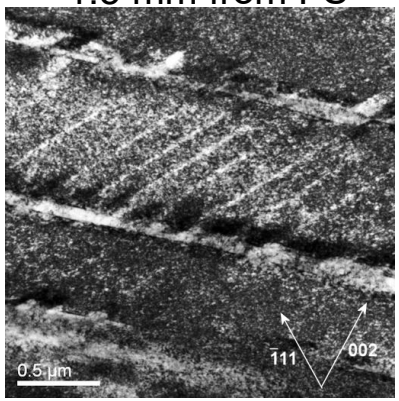

Argon, 340 ˚C
2 mm from FS

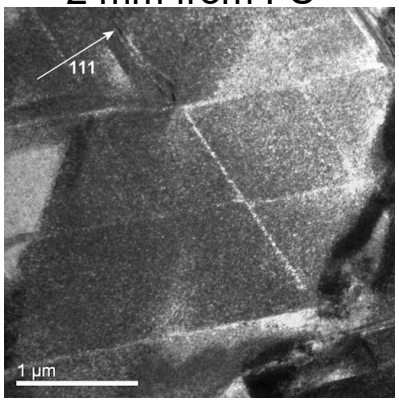

Argon, 340 ˚C
15 mm from FS

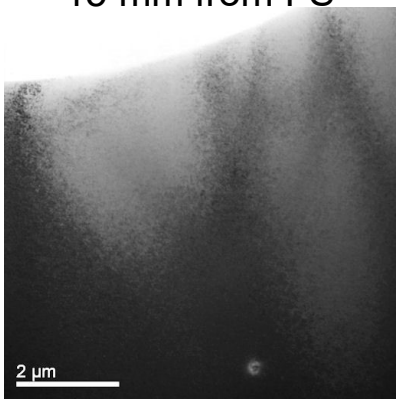

C10

PWR, 340 ˚C
0.5 mm from FS

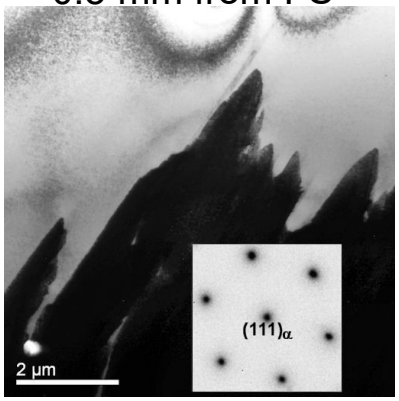

PWR, 340 ˚C
0.5 mm from FS

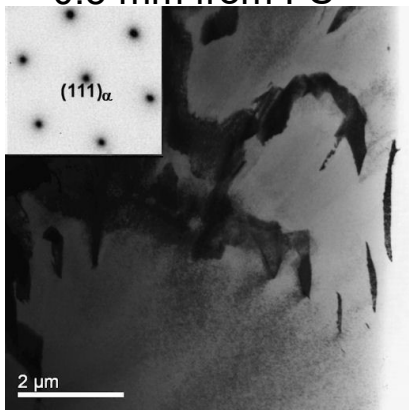

PWR, 340 ˚C
0.5 mm from FS

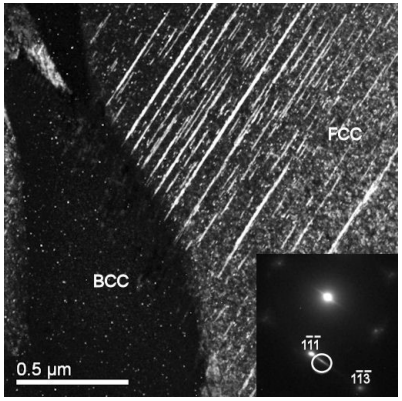

PWR, 340 ˚C
0.5 mm from FS

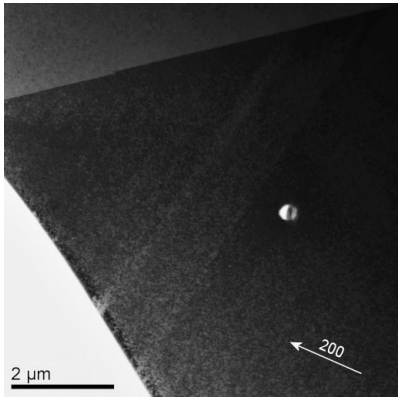

EU-PERFORM60 project (Grant Agreement: 232612)

IASCC example study: deformation

C4

PWR, 340 ˚C
1.5 mm from FS

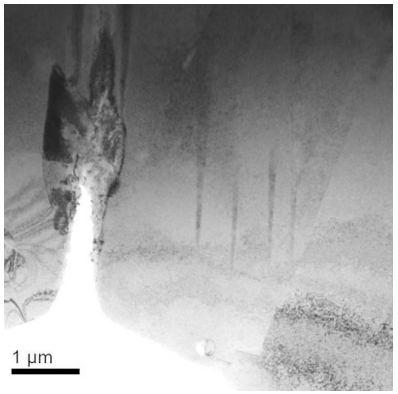

PWR, 340 ˚C
1.5 mm from FS

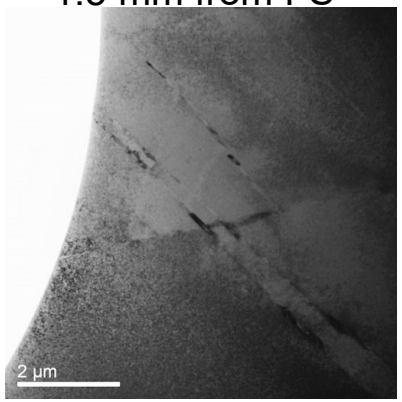

PWR, 340 ˚C
1.5 mm from FS

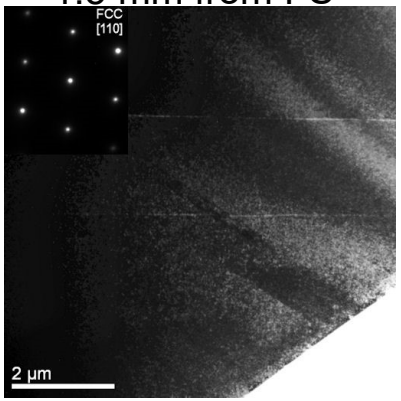

PWR, 340 ˚C
1.5 mm from FS

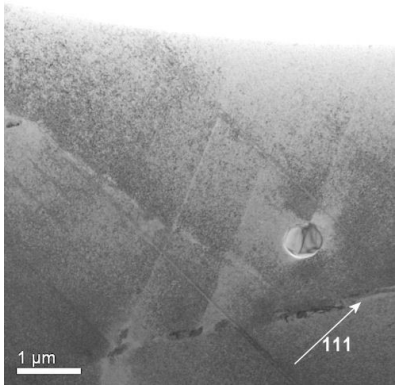

C5

Argon, 340 ˚C
0.5 mm from FS

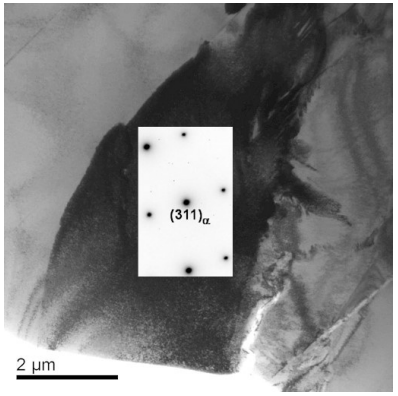

Argon, 340 ˚C
0.5 mm from FS

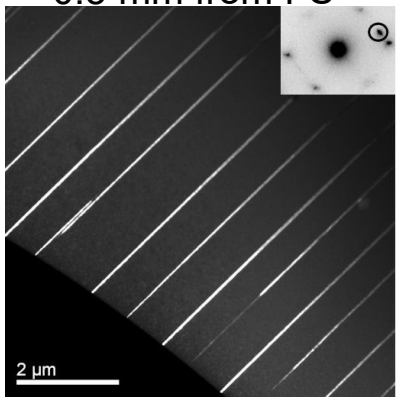

Argon, 340 ˚C
2 mm from FS

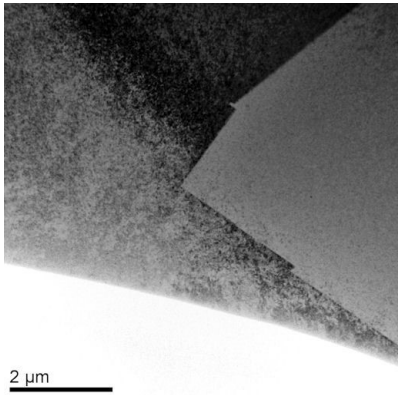

Argon, 340 ˚C
2 mm from FS

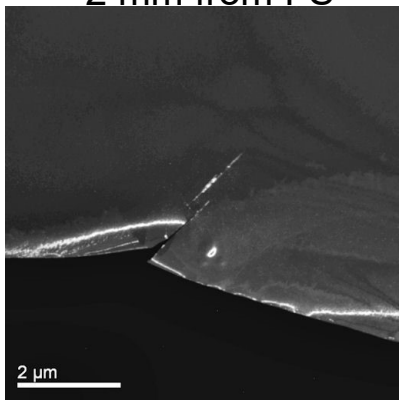

EU-PERFORM60 project (Grant Agreement: 232612)

IASCC example study; deformation

TEM specimen	Test bar	Distance from fracture	Deformation features
C4_2	C4 (CL)	1.5 mm	a few clear channels, a few small blooms of alpha martensite, but mostly no deformation
C5_1	C5 (CL)	0.5 mm	sparse population of twin-containing bands, a few small and large regions of alpha martensite
C5_2	C5 (CL)	2.0 mm	no deformation evident
C10_1	C10 (SSRT)	0.5 mm	one large region containing alpha martensite next to a region of closely-spaced stacking faults
C11_2	C11 (SSRT)	1.0 mm	heavy deformation in crisscrossing clear channels containing epsilon martensite and twins
C11_3	C11 (SSRT)	1.5 mm	significant deformation in crisscrossing clear channels containing some epsilon marteniste
C11_5	C11 (SSRT)	2.0 mm	deformation mostly in crisscrossing clear channels, some containing epsilon patches
C11_5	C11 (SSRT)	~ 15 mm	no deformation evident

EU-PERFORM60 project (Grant Agreement: 232612)

IASCC example study; deformation

- SSRT test conducted in argon produced substantial deformation through cleared channels, even 2 mm from the fracture surface, but the bar fractured in ductile manner.
- SSRT and CL tests in PWR environment and CL test in argon resulted in very little deformation product, even as close as 0.5 mm from the fracture surface, but showed significant IG fracture.
- Alpha martensite stood out as an interesting feature found at the proximity of the IG fracture surfaces.
- The combination of martensite and hydrogen may be an important factor in the IG fractures observed in this material.

Summary

- At low dpa, black-spot damage can promote localized deformation as **cleared channels**.
- With increasing dose (~3-10 dpa), faulted Frank loops are more prevelant, with average diameter <10 nm. Proton-irradiation also promoted loop formation.
- Proton-irradiation (5dpa at 350°C) produced Frank loops and nano-scale cavities; such cavity formation is typically observed after higher dose neutron irradiation.
- With a few (~3) dpa, grain boundary radiation-induced segregation becomes significant. Proton-irradiation to 5 dpa induced significant segregation to all defect sinks and grain boundaries.
- At high dpa (>10 dpa), significant radiation-induced precipitation of Ni- and Si-containing gamma prime occurs.
- At high dpa cavities can form, and can be associated with strong segregation of Ni and Si.
- As Ni is removed from matrix, austenite instability leads to easier transformation to alpha-prime martensite under loading.

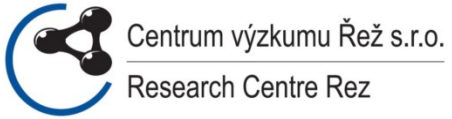

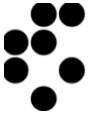

Institut "Jožef Stefan", Ljubljana, Slovenija

The SOTERIA Project Coordinator

Christian ROBERTSON
CEA
christian.robertson@cea.fr

The SOTERIA Project Office

Herman BERTRAND
ARTTIC
bertrand@arttic.eu

www.soteria-project.eu

This project received funding under the Euratom research and training programme 2014-2018 under grant agreement N° 661913.